



Machine learning methods for the study of cybersickness: a systematic review

Yang, A. H., Kasabov, N., & Cakmak, Y. (2022). Machine learning methods for the study of cybersickness: a systematic review. *Brain Informatics*, 9(1), 1-25. [24]. <https://doi.org/10.1186/s40708-022-00172-6>

[Link to publication record in Ulster University Research Portal](#)

Published in:
Brain Informatics

Publication Status:
E-pub ahead of print: 09/10/2022

DOI:
[10.1186/s40708-022-00172-6](https://doi.org/10.1186/s40708-022-00172-6)

Document Version
Publisher's PDF, also known as Version of record

General rights
Copyright for the publications made accessible via Ulster University's Research Portal is retained by the author(s) and / or other copyright owners and it is a condition of accessing these publications that users recognise and abide by the legal requirements associated with these rights.

Take down policy
The Research Portal is Ulster University's institutional repository that provides access to Ulster's research outputs. Every effort has been made to ensure that content in the Research Portal does not infringe any person's rights, or applicable UK laws. If you discover content in the Research Portal that you believe breaches copyright or violates any law, please contact pure-support@ulster.ac.uk.

REVIEW

Open Access



Machine learning methods for the study of cybersickness: a systematic review

Alexander Hui Xiang Yang¹, Nikola Kasabov^{2,3,4} and Yusuf Ozgur Cakmak^{1,5,6,7,8*}

Abstract

This systematic review offers a world-first critical analysis of machine learning methods and systems, along with future directions for the study of cybersickness induced by virtual reality (VR). VR is becoming increasingly popular and is an important part of current advances in human training, therapies, entertainment, and access to the metaverse. Usage of this technology is limited by cybersickness, a common debilitating condition experienced upon VR immersion. Cybersickness is accompanied by a mix of symptoms including nausea, dizziness, fatigue and oculomotor disturbances. Machine learning can be used to identify cybersickness and is a step towards overcoming these physiological limitations. Practical implementation of this is possible with optimised data collection from wearable devices and appropriate algorithms that incorporate advanced machine learning approaches. The present systematic review focuses on 26 selected studies. These concern machine learning of biometric and neuro-physiological signals obtained from wearable devices for the automatic identification of cybersickness. The methods, data processing and machine learning architecture, as well as suggestions for future exploration on detection and prediction of cybersickness are explored. A wide range of immersion environments, participant activity, features and machine learning architectures were identified. Although models for cybersickness detection have been developed, literature still lacks a model for the prediction of first-instance events. Future research is pointed towards goal-oriented data selection and labelling, as well as the use of brain-inspired spiking neural network models to achieve better accuracy and understanding of complex spatio-temporal brain processes related to cybersickness.

Keywords: Cybersickness, Detection, Prediction, Biometrics, Physiological, Review, Systematic, Machine learning, AI, Neural networks, Virtual reality, Extended reality, Simulator

1 Introduction

Cybersickness is a type of visually induced motion sickness experienced in virtual environments [1]. It is well-recognized that the symptoms of nausea, dizziness, fatigue and oculomotor problems have been a barrier to mainstream adoption of VR technology [1]. The utility of VR includes not just gaming and entertainment [2], but applications for professional training in healthcare, aerospace, industrial, defence, disaster safety and emergency procedures [3]. VR can also be used for planning cost-effective architectural designs [4]. Moreover, there

is potential for VR well-being applications in high-stress reduction [5], exposure therapy to reduce anxiety and trauma [6, 7] and health-related interventions using VR neuromodulation [8]. The importance of VR is further highlighted in environments with restricted social interactions such as those imposed by the recent COVID-19 pandemic, allowing people to connect despite physical boundaries [9]. Clearly, the world is progressing towards an integrated metaverse, which embraces immersive mixed realities [10]. It is, therefore, crucial to tackle the issue of cybersickness.

While visible physiological signs can be tell tales of an ongoing cybersickness event, it is still a perceptual disorder that is not always apparent until it is communicated [11]. Machine learning provides a way to log

*Correspondence: yusuf.cakmak@otago.ac.nz

¹ Department of Anatomy, University of Otago, Dunedin, New Zealand
Full list of author information is available at the end of the article

cybersickness events without overreliance on communication from VR users. This information enables timely prevention and treatment. The source of which comes from widely available sensor technology, which allows features to be derived from biometric and physiological data.

Measures include:

- Electrical activity in the brain [12–27]
- Electrical potentials of eye movement [25, 28, 29]
- Heart rate and heart rate variability [28, 30, 31]
- Gastric activity [25, 29]
- Muscle activity [24]
- Respiration rate [25, 28–32]
- Skin conductivity [28–31, 33]
- Eye blinks [25, 28, 29]
- Body movements [25, 34, 35]

Recently, Yildirim [36] reviewed four studies that used deep learning of electroencephalogram (EEG) data for the classification of cybersickness. The studies presented promising results, with accuracies in the range of 83.33–99.12% [36]. The review noted that extra care should be taken to report EEG data transformations, or lack thereof, as part of pre-processing. In addition, it was recommended that studies report clear descriptions for deep learning architectures, such as tensor shape, number and type of layers, activation functions and hyperparameters.

Moving forward, several other aspects in the wider literature require clarification. Across studies, there is a lack of homogeneity with regard to the definitions of detection and prediction. It is important to distinguish between the two to be clear about the extent of a machine learning model's capability. In this review, we define detection as the identification of data related to an ongoing cybersickness event. In contrast, we define prediction as the forecasting of future cybersickness using data prior to the event.

From a clinical perspective, the course of action against cybersickness would differ depending on the ability to detect or predict it. A model that detects cybersickness provides an opportunity for timely intervention, whereas a model that predicts potentially allows for early prevention.

A machine learning model's applicability is heavily dependent upon the data fed into it. Therefore, further investigation into the experimental design, method of data selection and data labelling in studies is needed. In addition, subject demographics, immersion environment and participant activity all influence the data obtained and the features extracted; ultimately framing the context of a model's results. An overview of these items across published studies is required, particularly to help future studies have clear goal implementation when designing an experiment or machine learning architecture.

Finally, cybersickness is a result of dynamic spatio-temporal processes in the brain, involving different spatially located areas over time [37, 38]. Appropriate machine learning (ML) methods can help provide a better understanding of these processes, at both the group and individual level, but this has not been clearly assessed yet in previous studies.

The goal of this systematic review was to analyse relevant studies pertaining to various physiological and biometric-based machine learning approaches towards the detection and prediction of cybersickness. The review provides a discussion of the experimental methods for data collection, processing and machine learning analysis within different architectures. In addition, suggestions for future exploration are discussed.

The research questions for this review are as follows:

1. How have studies been able to detect or predict cybersickness?
2. What stimulus type, environment and participant activity contributed towards cybersickness induction?
3. How are the reviewed articles comparable?
4. Which features are the most important?
5. What new information about brain activities related to cybersickness have been revealed by the studies?

1.1 Contributions

In summary, according to the research questions, we contribute the following:

- An in-depth summary of study design and details for each reviewed study
- A differentiation between prediction and detection studies
- Awareness of the consequences of mislabeling cybersickness data
- A highlight of the most informative features for machine learning and classification, with the caution they may not be generalizable or interpretable.
- Considerations for practical translation of machine learning algorithms to wearable devices for consumer usage, including number and type of sensors for different use cases.
- Future suggestions for machine learning of physiological data related to cybersickness.

Our justification for choosing these research questions and items of discussion, stems from the need to develop study protocols that properly capture cybersickness data according to specific research goals. The aspects chosen influence the type of data processed and are crucial to the

meaning of machine learning outputs. Furthermore, this affects not just the practical translatability of machine learning algorithms, but also the explainability of models that pave the way for the generation of new knowledge about cybersickness. Deliberation on these aspects will not only help to develop better study designs, but also aid in human adaptation to digital environments.

2 Methods

2.1 Database search

PubMed and IEEE Xplore databases were used to cover the intersection between biomedical and life sciences literature with that of computer science and engineering. Google Scholar was used to manually screen papers from an extensive array of journals and conferences based on their titles and abstracts. The review was written with PRISMA guidelines [39] for systematic reviews in mind. Eligible publications needed to utilize a stimulus to induce cybersickness through a virtual visual medium, such as either a screen projection, desktop display, VR head-mounted device or simulator environment. Publications also needed to apply machine learning on physiological data or physical measures of body and eye movement for the classification of cybersickness data samples. We define a study to be an instance of machine learning even if it solely uses regression analysis. Studies were excluded if an analysis was applied for knowledge

discovery about physiological correlations with cybersickness without any event detection, prediction or estimation of sickness levels. Studies analyzing only non-physiological data such as VR content or subjective questionnaire scores were excluded. Other exclusions were reviews, methodological articles, conference abstracts, and publications, where full-text was not available through our institutions. See Table 1 for the database search and selection criteria.

This review included all studies from 2001 to 10th November 2021. The search strategy was adapted from PICO criteria (Patient or population, Intervention, Control or Comparison, Outcome and Study; Table 2).

2.2 Search terms

Cybersickness OR visually induced motion sickness OR simulator sickness AND physiological AND machine learning AND Virtual Reality.

2.3 Screening process

Titles and abstracts of potential studies were assessed independently by three reviewers (AHX Yang, N. Kasabov, YO. Cakmak), according to the Preferred Reporting Items for Systematic Reviews and Meta-Analysis (PRISMA) guidelines [40]. The studies that met the inclusion and exclusion criteria were discussed and evaluated based on their content relative to the five research

Table 1 Database search and selection criteria

| Database search | |
|---------------------|--|
| Electronic database | 1. Pubmed 2. Google Scholar 3. IEEE Xplore |
| Inclusion criteria | 1. Articles that develop or validate a prediction or detection model using any data source, e.g., individual patient data or from electronic records 2. Studies must utilize a stimulus with a virtual visual medium 3. Any machine learning analysis and physiological processing or physical measures of body/eye movement collected from wearable devices for the classification of cybersickness 4. All outcome measures in any format, e.g., continuous, binary, ordinal, multinomial, time-to-event |
| Exclusion criteria | 1. Studies using machine learning to classify only non-physiological data, e.g., VR content or questionnaire scores 2. Studies that only investigate physiological correlations with cybersickness as a form of knowledge discovery 3. Reviews, Concept papers and abstracts 4. Full text not available |

Table 2 Search strategy

| Search strategy | |
|-----------------|--|
| Population | Studies using physiological data to build cybersickness classification algorithms |
| Intervention | Inducement of cybersickness to create labelled data for classification |
| Comparison | Different models and their utility for clinical intervention |
| Outcome | Ability to detect or predict cybersickness |
| Study type | Quantitative study |
| Keywords | Cybersickness OR visually induced motion sickness OR simulator sickness AND physiological AND machine learning AND virtual reality |

questions outlined above. Two reviewers (AHX Yang, YO. Cakmak) evaluated the full-text studies independently, while the third reviewer (N. Kasabov) resolved disagreements.

2.4 Data extraction and analysis

An initial risk of bias (ROB) assessment was run, from a conservative viewpoint. The ROB covered four domains from the PROBAST recommendations each containing their own signalling question items to judge risk of bias [41].

Responses were formulated as yes (Y) or probably yes (PY) for the absence of bias and no (N), probably no (PN), or no information (NI) to indicate a potential for bias. Overall judgement of risk of bias for publications was defined as high, low, or unclear. Although it is important to note that bias in itself is not necessarily a criticism of the choice of study design, which could be scientifically reasoned, but an assessment of erroneous

assumptions that may lead to misleading conclusions based on machine learning results.

Additional data items were extracted to answer the five research questions outlined above which are specific to the field of cybersickness classification. The data items include subject demographics, immersion type, participant activity, information on different machine learning models, reporting styles, data segment labelling, preprocessing methods, biometric and neurophysiological features relevant to cybersickness and EEG specifications. These data items are listed in Tables 3, 4, 5, 6, 7, 8, and 9, which sort studies by year from earliest to most recent. Two reviewers (AHX Yang, YO. Cakmak) independently extracted and assessed the data from the included studies, while the remaining reviewer (N. Kasabov) cross-referenced, clarified differences in interpretation, and then confirmed a standardized response. Any disagreements reached a consensus and were resolved by the third reviewer (N. Kasabov) after discussion.

Table 3 Subject demographic including sample size, gender, age range and mean with standard deviation where available

| Author | N | Male | Female | Age range | Mean |
|-----------------------------|----------------------|------|--------|-----------|--------------|
| <i>Subject demographics</i> | | | | | |
| Nam et al. [12] | 45 | 25 | 20 | 18–26 | 21.9 |
| Yu et al. [13] | 7 | – | – | 21–24 | – |
| Wei et al. [16] | 6 | – | – | – | – |
| Wei et al. [14] | 6 | – | – | – | – |
| Ko et al. [15] | 10 | – | – | – | – |
| Lin et al. [17] | 10 | – | – | – | – |
| Ko et al. [18] | 6 | – | – | – | – |
| Lin et al. [19] | 17 | – | – | – | – |
| Dennison et al. [29] | 20 (9 completed) | 14 | 6 | – | – |
| Pane et al. [26] | 9 | 6 | 3 | 25–35 | – |
| Mawalid et al. [21] | 9 | 7 | 2 | – | – |
| Khoirunnisaa et al. [20] | 9 | 7 | 2 | – | 25.1 |
| Dennison et al. [25] | 20 | 15 | 5 | > 18 | – |
| Wang et al. [34] | 11 | 7 | 4 | – | 25.83 ± 4.58 |
| Garcia-Agundez et al. [28] | 66 | – | – | – | – |
| Jeong et al. [22] | 24 | 13 | 12 | 20–33 | – |
| Li et al. [35] | 20 | 20 | 0 | 18–27 | 22.8 |
| Kim et al. [42] | 202 | – | – | – | – |
| Liao et al. [27] | 130 | 65 | 65 | 6–23 | – |
| Li et al. [23] | 18 (6 excluded) | 19 | 5 | – | 29.3 |
| Lee, Alamaniotis [43] | 31 | 29 | 2 | – | 24.04 ± 2.75 |
| Islam et al. [30] | 31 (8 excluded) = 23 | 29 | 2 | – | 24.04 ± 2.75 |
| Islam et al. [31] | 31 (8 excluded) = 23 | 29 | 2 | – | 24.04 ± 2.75 |
| Martin et al. [33] | 103 | 86 | 17 | – | 26.12 ± 6.31 |
| Recenti et al. [24] | 28 | 22 | 6 | – | 23.8 ± 1.2 |
| Oh, Kim [32] | 20 (2 excluded) = 18 | 8 | 12 | – | – |

Dashes (–) are put, where information was missing or not available

Table 4 Immersion type including mode of stimulus, VR content, platform usage, and participant activity

| Author | Mode of stimulus | VR content | Platform (moving/still) | Standing/sitting/active |
|--|---|---------------------------------------|-----------------------------|--|
| <i>Immersion type and participant activity</i> | | | | |
| Nam et al. [12] | 3D virtual environment simulator | Virtual background of buildings | None | Unclear |
| Yu et al. [13] | 360 degree Simulator, 6 degrees freedom motion platform | Auto driving | Moving, sync with simulator | Passive sitting (visual + vestibular) |
| Wei et al. [16] | 360 degree Simulator, 6 degrees freedom motion platform | Auto driving | Moving, sync with simulator | Passive sitting (visual + vestibular) |
| Wei et al. [14] | 360 degree Simulator, 6 degrees freedom motion platform | Auto driving | Moving, sync with simulator | Passive sitting (visual + vestibular) |
| Ko et al. [15] | 360 degree Simulator, 6 degrees freedom motion platform | Auto driving | Moving, sync with simulator | Passive sitting (visual + vestibular) |
| Lin et al. [17] | 360 degree Simulator, 6 degrees freedom motion platform | Auto driving | Moving, sync with simulator | Passive sitting (visual + vestibular) |
| Ko et al. [18] | 360 degree Simulator, 6 degrees freedom motion platform | Auto driving | Moving, sync with simulator | Passive sitting (visual + vestibular) |
| Lin et al. [19] | 360 degree Simulator, 6 degrees freedom motion platform | Auto driving | Moving, sync with simulator | Passive sitting (visual + vestibular) |
| Dennison et al. [29] | Display Monitor 1920 × 1280 resolution, Oculus Rift | VR exploration | None | Passive sitting (visual) |
| Pane et al. [26] | 47 Inches LED Monitor HD-1366 × 768 resolution | Mirrors edge | None | Sitting (active playing, visual) |
| Mawalid et al. [21] | 47 Inches LED Monitor HD-1366 × 768 resolution | Mirrors edge | None | Sitting (active playing, visual) |
| Khoirunnisaa et al. [20] | 47 Inches LED Monitor HD-1366 × 768 resolution | Mirrors edge | None | Sitting (active playing, visual) |
| Dennison et al. [25] | Oculus rift DK2 | VR exploration | None | Standing (visual) |
| Wang et al. [34] | HTC Vive HMD | Virtual exploration | None | Standing (visual) |
| Garcia-Agundez et al. [28] | Oculus rift DK2 | VR plane flying | None | Active sitting (visual) |
| Jeong et al. [22] | FOVE VR headset | 6 VR videos | None | Unclear |
| Li et al. [35] | Projected screen | Forward/backward video, auto driving | None | Standing (visual) |
| Kim et al. [42] | HTC vive HMD | 44 VR videos | None | Unclear |
| Liao et al. [27] | HTC vive HMD | Roller coaster, space simulator, boat | None | Passive sitting (visual) |
| Li et al. [23] | HTC vive HMD | VR roaming | None | Passive sitting (visual) |
| Lee and Alamaniotis [43] | HTC vive HMD | VR rollercoaster | None | Passive sitting (visual) |
| Islam et al. [30] | HTC vive HMD | VR rollercoaster | None | Passive sitting (visual) |
| Islam et al. [31] | HTC vive HMD | VR rollercoaster | None | Passive sitting (visual) |
| Martin et al. [33] | Oculus rift | Multiple VR games | None | Active sitting (visual) |
| Recenti et al. [24] | VR Goggles HMD + moving platform | Open sea boat on waves | Moving, sync with VR waves | Standing in all stages, active balancing (visual + vestibular) |
| Oh and Kim [32] | HTC vive HMD | VR rollercoaster | None | Passive sitting (visual) |

3 Results

3.1 Search and Selection

The database search identified 446 studies. After manual screening for titles and abstracts, 40 studies

remained based on the inclusion/exclusion criteria. 14 studies were further excluded upon assessment of the full text. Among them, there were 2 reviews, 2 concept papers, 2 duplicates, 3 did not use machine learning for

Table 5 Biosignal recordings, machine learning algorithms, performance and type of classification system in terms of detection or prediction

| Authors | Biosignal | Algorithm | Binary/multiclass | Accuracies | Classification type |
|--------------------------------|--|---|-----------------------------------|--|---------------------|
| <i>Machine learning models</i> | | | | | |
| Nam et al. [12] | EEG, EOG, ECG, finger tip skin temperature, PPG, skin conductance | ANN, 2-layer feedforward neural network | Binary | Minimum mean square error 0.092 | Detection |
| Yu et al. [13] | EEG | GMLC, KNN, SVM | Binary | KNN, NWE 99.9% | Detection |
| Wei et al. [16] | EEG | RBFNN, SVR, LR | Multi class motion sickness level | 84.07% LR 84.75% RBFNN, 86.92% SVR | Detection |
| Wei et al. [14] | EEG | RBFNN | Multi class motion sickness level | 84.39% \pm 0.75 | Detection |
| Ko et al. [15] | EEG | LR, PCR | Multi class motion sickness level | PCR 78.3% \pm 8.0 LR 64.7% \pm 15.6 | Detection |
| Lin et al. [17] | EEG | SVM | Multi class motion sickness level | 36.3–73.3% | Detection |
| Ko et al. [18] | EEG | SVM | Multi class motion sickness level | 58.5–97.0% | Detection |
| Lin et al. [19] | EEG | SONFIN, LR, SVR | Multi class motion sickness level | Broad band EEG SONFIN 82% \pm 2 SVR 79% \pm 3 LR 80% \pm 3 | Detection |
| Dennison et al. [29] | ECG, EEG, EOG, blink rate, PPG, breathing rate, GSR | Stepwise regression | SSQ score estimation | Adjusted R^2 : Cybersickness 0.296 Nausea 0.101 Oculomotor 0.674 Disorientation 0.268 | Detection |
| Pane et al. [26] | EEG | CN2 rule induction algorithm, decision tree, SVM | Multiclass | CN2 88.9% Decision tree 72.2% SVM 83.3% | Detection |
| Mawalid et al. [21] | EEG | Naïve Bayes, KNN | Binary | KNN 83.3% Naïve bayes 88.9% | Detection |
| Khoirunnisaa et al. [20] | EEG | SVM-RBF, KNN, LDA | Binary | SVM-RBF 83.3% KNN 83.0% LDA 100% | Detection |
| Dennison et al. [25] | EEG, ECG, EOG, blink rate, breathing rate, EGG, postural sway, head movement | LDA, KNN, Naïve Bayes, decision tree, ADABOOSTM2, and bagged decision trees | Multiclass | Unimodal Feature Bag classifier: EEG: 93.80% Posture: 83.48% Breathing rate: 81.32% HMD sensors: 78.40% Avatar movement: 74.40% ECG: 68.44% EOG: 61.84% EGG: 48.52% Multimodal feature fusion: Bag: 95% KNN: 93% ADABOOST: 92% | Detection |

Table 5 (continued)

| Authors | Biosignal | Algorithm | Binary/multiclass | Accuracies | Classification type |
|----------------------------|---|---|---|--|--------------------------|
| Wang et al. [34] | Postural sway | LSTM | SSQ score estimation | Pearson correlation coefficient $r = 0.89$ between SSQ score and loss (measure of difference in postural sway between pre and post VR exposure) | Detection |
| Garcia-Agundez et al. [28] | ECG, EOG, blink rate, breathing rate, GSR | Fine Gaussian SVM, linear SVM, KNN | Binary and Multiclass | Binary: fine Gaussian SVM: no cs: 57.6%, minor: 74.2%, severe: 81.8% Ternary: KNN: 58% DNN 98.02% CNN 98.82% | Detection |
| Jeong et al. [22] | EEG | DNN, CNN | Binary cutoff | single subject binary classification: 91.1% multiple subject binary classification: 76.3% 3 class classification: 86.7% Severe, 50.4% moderate, 79.1% mild, 68.9% average accuracy | Detection |
| Li et al. [35] | EEG, postural sway, head body movement | KNN, LR, RF, MLP in a voting classifier | Multiclass | LSTM with EEG $87.13\% \pm 1.51$ Combined LSTM EEG + CNN-RNN visual features: $89.16\% \pm 1.87\%$ visual predictor alone: $79.03 \pm 1.24\%$ | Detection |
| Kim et al. [42] | EEG | CNN, LSTM, RNN | Multiclass | 1 min: 83.94%, 5-min 83.33%, 10 min 83.92% 82.83% for RNN-LSTM, CNN at 73.13%. MLP at 71.31% and Lib-SVM at 62.58% | Prediction |
| Liao et al. [27] | EEG | LSTM, SVM, MLP, CNN | Binary cutoff custom sickness index | Single subject binary classification: polynomial-SVM 92.83%, KNN 90.97%, RBF-SVM 90.74% Multiple subject classification: 79.25%, 77.5%, 73.84%, respectively | Detection |
| Li et al. [23] | EEG | KNN, polynomial-SVM, RBF-SVM | Binary | DESOM Purity index 96.87% | Prediction |
| Lee and Alamaniotis [43] | EEG | DESOM with auto encoder for clustering, KNN | Binary | MAE 8.7% Detection: 97.44%, Prediction: 87.38% | Prediction |
| Islam et al. [30] | ECG, breathing rate, GSR | LSTM regression analysis | Multiclass | | Detection and Prediction |
| Islam et al. [31] | ECG, breathing rate, GSR | CNN-LSTM | Multiclass based on sickness score estimation | | |

Table 5 (continued)

| Authors | Biosignal | Algorithm | Binary/multiclass | Accuracies | Classification type |
|---------------------|-------------------------|--|---|---|---------------------|
| Martin et al. [33] | BVP, EDA | SVM, GB, RF, LR | Sickness rating estimation, Binary and Multiclass | Model trained on all participants: LR: R^2 0.75 RF: binary 91.7%, multiclass 86.2% One model for each participant: LR: R^2 0.40 RF: binary 89%, multiclass 85.9% | Prediction |
| Recenti et al. [24] | EEG, EMG, heart rate | RF, GB tree, SVM, KNN, MLP | Binary | RF: IPV 75.9%, INM, 79.5%, IMS 74.7% | Detection |
| Oh and Kim [32] | BVP, respiratory signal | DELM with SVM, KNN, RF, ADA-boost stacked into CNN | Multiclass | SVM: 94.23%, KNN: 92.44%, RF: 93.20%, ADABOOST: 90.33%, DELM: 96.48% | Detection |

For simplicity, relevant top accuracies/results are reported. Artificial neural network (ANN) gaussian maximum likelihood classifier (GMLC), k-nearest neighbour (KNN), support vector machine (SVM), radial basis function neural network (RBFNN), support vector regression (SVR), linear regression (LR), principal component regression (PCR), self-organizing neural fuzzy inference network (SONFIN), linear discriminant analysis (LDA), long short-term memory (LSTM), Deep neural network (DNN), convolutional neural network (CNN), multilayer perceptron (MLP), deep embedded self-organizing map (DESON), random forest (RF), deep ensemble learning model (DELM) IPV (physiological index), INM (neurological/muscle strain index), IMS (motion sickness index), mean absolute error (MAE), non-parametric weighted feature extraction (NFWE)

Table 6 Reporting styles and data labelling

| Author | Biosignal | Report | Non-cybersickness labelling | Cybersickness labelling |
|----------------------------|--|------------------------------|--|--|
| Nam et al. [12] | EEG, EOG, ECG, finger tip skin temperature, PPG, skin conductance | Verbal | Data points not labelled as cybersick | Within 3 s of report while immersed |
| Yu et al. [13] | EEG | Joystick scale | Participant defined time segments | Continuous scale |
| Wei et al. [16] | EEG | Joystick scale | Participant defined time segments | Continuous scale |
| Wei et al. [14] | EEG | Joystick scale | Participant defined time segments | Continuous scale |
| Ko et al. [15] | EEG | Joystick scale | Participant defined time segments | Continuous scale |
| Lin et al. [17] | EEG | Joystick scale | Participant defined time segments | Continuous scale |
| Ko et al. [18] | EEG | Joystick scale | Participant defined time segments | Middle of motionsickness level graph and after highest sickness rating |
| Lin et al. [19] | EEG | Joystick scale | Participant defined time segments | Continuous scale |
| Dennison et al. [29] | ECG, EGG, EOG, blink rate, PPG, breathing rate, GSR | SSQ | N/A (SSQ score estimation) | Entire VR immersion |
| Pane et al. [26] | EEG | SSQ cut-off score | Before gameplay | Tailend of gameplay |
| Mawalid et al. [21] | EEG | SSQ cut-off score | Before gameplay | tailend of gameplay |
| Khoirunnisaa et al. [20] | EEG | SSQ cut-off score | Before gameplay | total gameplay |
| Dennison et al. [25] | EEG, ECG, EOG, blink rate, breathing rate, EGG, postural sway, head movement | In game input via controller | Score of zero for 'no symptoms' on a zero to three point scale | 30 s intervals |
| Wang et al. [34] | Postural sway | SSQ | N/A (SSQ score estimation) | N/A (SSQ score classification) |
| Garcia-Agundez et al. [28] | ECG, EOG, blink rate, breathing rate, GSR | SSQ | SSQ score cut off | Entire VR immersion |
| Jeong et al. [22] | EEG | Keyboard marker | Unclear | entire video |
| Li et al. [35] | EEG, postural sway, head body movement | Keyboard marker | During VR, before video movement | Varying interval throughout video |
| Kim et al. [42] | EEG | Likert scale | Video contents scored '1: comfortable' on Likert-like scale | Mid video |
| Liao et al. [27] | EEG | Verbal | Lack of cybersickness report during VR immersion | Report of sickness, entire recording |
| Li et al. [23] | EEG | Tact switch | Before VR immersion | Varying interval throughout immersion |
| Lee and Alamaniotis [43] | EEG | Mouse click | During VR, before video movement | 2 s timespan, 1 s before cybersickness report |
| Islam et al. [30] | ECG, breathing rate, GSR | Verbal | Sickness scale cutoff for entire VR immersion | Sickness scale cutoff for entire VR immersion |
| Islam et al. [31] | ECG, breathing rate, GSR | Verbal | Before VR immersion, and before video movement | Entire VR immersion |
| Martin et al. [33] | BVP, EDA | Verbal | Score of zero on VR sickness scale | Window sizes of 10, 30, 60, 90, 120 s before report of sickness with a score equal to or more than 1 |
| Recenti et al. [24] | EEG, EMG, heart rate | MSSQ | N/A (index classification) | N/A |
| Oh and Kim [32] | BVP, respiratory signal | Verbal | no report of cybersickness and pre-immersion neutral states | Entire VR immersion |

Simulator sickness questionnaire (SSQ), motion sickness questionnaire (MSSQ)

Table 7 Preprocessing methods

| Author | Biosignal | Preprocessing |
|------------------------------|--|---|
| <i>Preprocessing methods</i> | | |
| Nam et al. [12] | EEG, EOG, ECG, finger tip skin temperature, PPG, skin conductance | Power band extraction, standard deviation of EOG, mean R–R of ECG, mean and standard deviation of fingertip skin temperature, PPG and skin conductivity. Data segments for all variables calculated in period 3 (30 s after to the end of VR immersion) ratioed to period 1 and 2 (1 min before VR immersion and 30 s after) |
| Yu et al. [13] | EEG | 1–50 Hz high and low pass filter, 250 Hz down sampling, ICA, component clustering, FFT and conversion to decibel power |
| Wei et al. [16] | EEG | 1–50 Hz high and low pass filter, 250 Hz down sampling, ICA, component clustering, FFT and conversion to decibel power |
| Wei et al. [14] | EEG | 1–50 Hz high and low pass filter, 250 Hz down sampling, ICA, component clustering, FFT and conversion to decibel power |
| Ko et al. [15] | EEG | 1–50 Hz high and low pass filter, 250 Hz down sampling, ICA, component clustering, FFT and conversion to decibel power |
| Lin et al. [17] | EEG | 1–50 Hz high and low pass filter, 250 Hz down sampling, ICA, component clustering, FFT for PSD and subsequent conversion to decibel power |
| Ko et al. [18] | EEG | 1–50 Hz high and low pass filter, 250 Hz down sampling, ICA, component clustering, FFT for PSD and conversion to decibel power |
| Lin et al. [19] | EEG | 1–50 Hz high and low pass filter, 250 Hz down sampling, ICA, component clustering, FFT for PSD and conversion to decibel power |
| Dennison et al. [29] | ECG, EGG, EOG, blink rate, PPG, breathing rate, GSR | ECG bandpass filter 0.5–30 Hz, EGG bandpass filter 0.005–2 Hz and FFT with Hamming window, percentage band power for tachygastic and bradygastic activity, respiration bandpass filter 0.1–1 Hz, PPG bandpass filter 0.1–10 Hz, EOG bandpass filter 0.1–5 Hz, baseline normalization for skin conductivity, standard deviation of yaw, pitch and roll head rotation in degrees |
| Pane et al. [26] | EEG | FIR bandpass 1–40 Hz, ICA, ratio logarithmic of PSD (percentage power), change in percentage power pre-stimuli to post stimuli (percentage change) Daubechies 4 wavelet (db4) function |
| Mawalid et al. [21] | EEG | ICA, Chebyshev bandpass filter type II |
| Khoirunnisaa et al. [20] | EEG | FIR bandpass 1–40 Hz, ICA, Discrete Wavelet transform, Welch's method for PSD |
| Dennison et al. [25] | EEG, ECG, EOG, blink rate, breathing rate, EGG, postural sway, head movement | ECG bandpassfilter 0.5–30 Hz, EEG bandpass filter 0.1–30 Hz, data interpolation from other channels after manual artifact removal, ICA, FFT, EOG bandpass filter 0.1–5 Hz, EGG bandpass filter 0.005–2 Hz, FFT with Hamming window, percentage band power for tachygastic and bradygastic activity, respiration bandpass filter 0.1–1 Hz, standard deviation of yaw, pitch and roll rotation degrees, average and standard deviations in weight changes for postural sway. Any missing data replaced and standardized across features |
| Wang et al. [34] | Postural sway | – |
| Garcia-Agundez et al. [28] | ECG, EOG, blink rate, breathing rate, GSR | Mean and standard deviation on game content vectors |
| Jeong et al. [22] | EEG | 4–45 Hz automatic filter. Data sets created based on 4 custom signal quality weightings, min max normalization/standardization |
| Li et al. [35] | EEG, postural sway, head body movement | Channel integration, paired interception, simultaneous artifact removal, FFT for PSD |
| Kim et al. [42] | EEG | Bandpass filter 0.3–100 Hz, notch filter at 60 Hz, FFT applied through a sliding Hann window. EEG Data transformed into a 8 channel stacked spectrogram |
| Liao et al. [27] | EEG | FFT for PSD |

Table 7 (continued)

| Author | Biosignal | Preprocessing |
|--------------------------|--------------------------|---|
| Li et al. [23] | EEG | Elliptical pass band filter 0.5–30 Hz, Fourier transform, 7 level WPT |
| Lee and Alamaniotis [43] | EEG | 256 Hz down sampling |
| Islam et al. [30] | ECG, breathing rate, GSR | z-score removal of outliers |
| Islam et al. [31] | ECG, breathing rate, GSR | z-score removal of outliers, 1 Hz down sampling, min–max normalization |
| Martin et al. [33] | BVP, EDA | BVP inter-beat interval extraction bandpass filter 0.66–3.33 Hz, frequency and time domain feature computation, EDA tonic and phasic computation |
| Recenti et al. [24] | EEG, EMG, heart rate | 0.1–40 Hz high pass and low pass filter, 300 microvolts upper limit, common average reference, interpolation for removed channels, baseline correction, DC offset correction, Welch's method for PSD, relative power averaged across all channels |
| Oh and Kim [32] | BVP, respiratory signal | Exclusions of data samples after inspection for artifacts |

Independent component analysis (ICA), fast Fourier transform (FFT), power spectral density (PSD), wavelet packet transform (WPT), direct current (DC)

classification and 5 did not analyze biometric or physiological signals. The remaining 26 papers were included in this review. Figure 1 presents a flowchart of the study screening and selection process.

3.2 Risk of Bias

All studies had an overall low risk of bias (see Table 10). Of these, one study [27] had a “No” for item 17, because data segments were labelled as cybersick that may have contained control data. Another study [23] sampled control data that may have been influenced by conditions other than the lack of cybersickness, such as non-VR immersion. One study [12] had “No” for item 14, because only participants who felt nausea were used and “NI” for 15 and 19, because it was unclear if there were missing data or if the model accounted for overfitting. Most studies (21/26), had a low participant sample size (item 12). Two studies [15, 17] had a “No” for items 3 and 5 as they employed feature selection algorithms that differed among participants. Eleven studies (see Table 10) were either unclear, or did not report exclusion of participants with health disorders (item 2) which could affect the feature variables used in classification of cybersickness and even contribute to already having nausea, although this was not weighted as heavily in the overall ROB assessment.

3.3 Subject demographics

The sample size of subjects ranges from 6 to 202 throughout the 26 studies. Of the 26 studies, 17 report gender, and 9 do not. Most of the studies consist of predominantly male participants, while one study uses comparatively more females [32] and a few balance both male and female participants [12, 22, 27]. With regard to age reporting, 15 out of 26 studies report ages, of which 12 studies either report the age range or mean with standard deviation. For details, refer to Table 3.

3.4 Immersion type and participant activity

Both vestibular and visual stimuli or visual alone have been used. Visual mediums include 360° simulators, LED desktop display monitors, projected screens and head mounted displays (HMDS), refer to Table 4. Moving platforms have been incorporated, including ones that mimic sea waves on a ship [24] and automatic driving simulators [13–19], both of which introduce vestibular stimuli in synchronicity with their virtual environments. Studies have made participants play games [20, 21, 26, 28, 33], undergo virtual navigation [12, 23, 25, 34], or watch virtual videos [22, 27, 30–32, 35, 42, 43]. During these activities, there would doubtless exist some self-induced vestibular stimuli through head movements or balancing while standing. It is unclear in three studies whether a standing or sitting posture was used during either virtual simulator environment immersion or VR HMD usage while watching videos [12, 22, 42]. Each study's mode of stimulus, VR content, platform usage and type of participant activity are summarized in Table 4.

3.5 Machine learning models

Table 5 summarizes the machine learning analysis undertaken by all 26 studies. This includes biosignal recordings, algorithm(s) used, classification types in terms of binary, multiclass, or score estimation, accuracies, and abilities of models to detect or predict cybersickness. Out of all the studies, five have built predictive algorithms, while the rest have detected cybersickness [30, 27, 31, 33, 43].

3.6 Biosignals recorded

Studies have utilized electroencephalogram (EEG), electrooculography (EOG), electrocardiogram (ECG), photoplethysmography (PPG), electrogastrogram (EGG), electromyogram (EMG), Respiration signals, galvanic skin response (GSR) also known as electrodermal activity

Table 8 Feature extraction, selection methods, fusion with other biosignals for machine learning and the important features from each study

| Author | Biosignal | Feature extraction/selection methods | Feature fusion | Important features |
|--|--|--|----------------|---|
| <i>Biometric and neurophysiological features relevant to cybersickness</i> | | | | |
| Nam et al. [12] | EEG, EOG, ECG, finger tip skin temperature, PPG, skin conductance | PCA | Yes | Fz, Cz, Pz, O1, O2, theta (5–8 Hz), alpha (9–13 Hz), beta (14–30 Hz), gamma (31–50 Hz), standard deviation of EOG, mean R-R of ECG, mean and standard deviation of fingertip skin temperature, PPG and skin conductivity |
| Yu et al. [13] | EEG | PCA, LDA, NWFE, FFS/BFS for PSD | None | Delta (0.1–3 Hz), theta (4–7 Hz), alpha (8–13 Hz), beta (14–30 Hz) |
| Wei et al. [16] | EEG | PCA for PSD | None | Broadband frequency 1–50 Hz |
| Wei et al. [14] | EEG | Genetic algorithm for PSD | None | Broad band frequencies, especially delta (1–3 Hz), alpha (8–12 Hz), beta (13–30 Hz), channels unknown |
| Ko et al. [15] | EEG | PCA for PSD | None | Fp1, Fp2, C3, C4, Pz, Oz |
| Lin et al. [17] | EEG | Inheritable bi-objective combinatorial genetic algorithm (IBCGA) for PSD | None | Gamma band (21–50 Hz) (parietal area and occipital midline) |
| Ko et al. [18] | EEG | Extended inheritable bi-objective combinatorial genetic algorithm (e-IBCGA) for PSD | None | Beta (13–20 Hz) and gamma (21–30 Hz) (parietal area and occipital midline) |
| Lin et al. [19] | EEG | PCA for PSD | None | Alpha (8–12 Hz) and gamma (21–30 Hz) combined, broad band signals (occipital midline) |
| Dennison et al. [29] | ECG, EEG, EOG, blink rate, PPG, breathing rate, GSR | Pearson correlation with SSQ cut-off | None | Bradygastic (less than 2 cycles of contraction per minute) percentage power, mean blinks, mean breaths, MSSQA |
| Pane et al. [26] | EEG | ANOVA to rank frequency band feature importance based on 3 class labels (none, low, high cybersickness) | None | Decrease of Percentage power of beta (12–30 Hz) in O1 |
| Mawalid et al. [21] | EEG | Mean, variation, standard deviation, number of peak and ratio logarithmic of power spectral density (power percentage) | Yes | Alpha (8–13 Hz) and beta (13–20 Hz) combined for all 14 channels, as well as their variation and standard deviation |
| Khoirunnisaa et al. [20] | EEG | Channel selection through information gain and correlation-based on feature selection | None | Power percentage beta (16–32 Hz) for $F3 > O1 > O2 > F4 > AF4$ |
| Dennison et al. [25] | EEG, ECG, EOG, blink rate, breathing rate, EGG, postural sway, head movement | Greedy sequential forward feature selection process | Yes | Number of breaths per 30 s, number of blinks per 30 s, heart rate, ECG R-peak amplitude, avatar right-left displacement, % of slow wave stomach activity (less than 2 cycles of contraction per minute), 13 EEG powerband features (0.1–30 Hz) (left frontal alpha, left motor theta, left parietal beta, left occipital delta, left occipital theta, left occipital alpha, right frontal theta, right frontal gamma, right motor delta, right motor theta, right parietal beta, right parietal delta, and right occipital gamma) |
| Wang et al. [34] | Postural sway | LSTM encoder to learn features | No | Reconstruction error of postural sway signal |

Table 8 (continued)

| Author | Biosignal | Feature extraction/selection methods | | Feature fusion | Important features |
|----------------------------|---|--|------|----------------|--|
| Garcia-Agundez et al. [28] | ECG, EOG, blink rate, breathing rate, GSR | HR, breathing rate, respiration rate using peak detection algorithm | Yes | Yes | Combination of game content vectors, heart rate, blink rate, respiratory rate, galvanic skin response |
| Jeong et al. [22] | EEG | Raw data + power bands | Yes | Yes | Signal quality weightings |
| Li et al. [35] | EEG, postural sway, head body movement | PCA for Power band, centre of pressure, head and waist movement | Yes | Yes | Combination of theta (4–8 Hz) and alpha (8–13 Hz) in all 31 channels, center of pressure, head and waist movement |
| Kim et al. [42] | EEG | Temporal and spectral networks | Yes | Yes | P3, P4 |
| Liao et al. [27] | EEG | PSD | Yes | Yes | Broadband frequencies, 0–100 + Hz |
| Li et al. [23] | EEG | Combined 4 rhythm energy ratios for all channels | None | None | FP1, FP2, C3, C4, P3, P4, O1, O2 |
| Lee and Alamaniotis [43] | EEG | EEGNET to capture features | None | None | Unknown |
| Islam et al. [30] | ECG, breathing rate, GSR | Pearson-correlation coefficient analysis, min, max, running average for HR, HRV and GSR | Yes | Yes | Min, max, running average for heart rate, heart rate variability and galvanic skin response |
| Islam et al. [31] | ECG, breathing rate, GSR | Pearson-correlation coefficient analysis, min, max, running average for HR, HRV and GSR | Yes | Yes | Min, max, running average for heart rate, heart rate variability and galvanic skin response |
| Martin et al. [33] | BVP, EDA | HRV time domain and frequency domain computation, EDA tonic and phasic feature computation | Yes | Yes | Binary and multiclassification Rank 1/50: Baseline EDA minimum amplitude Binary classification only Rank 5/50: Heart rate Multiclassification only Rank 5/50: pNN50 |
| Recenti et al. [24] | EEG, EMG, heart rate | Power spectra based on previous studies | Yes | Yes | Beta EEG signals (13–35 Hz), EMG at right gastrocnemius 40–132 Hz, average HR |
| Oh and Kim [32] | BVP, respiratory signal | Manual selection of HRV and respiratory signal features | Yes | Yes | HR, HRV amplitude, LF, HF, and LF/HF ratio, respiratory rate and respiratory value |

Principle component analysis (PCA), linear discriminant analysis (LDA), non-parametric weighted feature extraction (NFWFE), forward feature selection (FFS), backward feature selection (BFS), power spectral density (PSD), simulator sickness questionnaire (SSQ), long short-term memory (LSTM), heart rate (HR), heart rate variability (HRV), galvanic skin response (GSR), electrodermal activity (EDA), low frequency (LF), high frequency (HF).

Table 9 EEG devices, channels and powerband frequencies

| Authors | Device | Channels used | Power band frequencies |
|---------------------------|---|--|---|
| <i>EEG specifications</i> | | | |
| Nam et al. [12] | Five channel 200 Hz sampling rate | Five channel EEG Fz, Cz, Pz, O1, O2 | Theta (5–8 Hz), alpha (9–13 Hz), beta (14–30 Hz), gamma (31–50 Hz) |
| Yu et al. [13] | Unknown, 32 channel | P8, T8, CP6, FC6, F8, F4, C4, P4, AF4, Fp2, Fp1, AF3, Fz, FC2, Cz, CP2, PO3, O1, Oz, O2, PO4, Pz, CP1, FC1, P3, C3, F3, F7, FC5, CP5, T7, P7 | Delta (0.1–3 Hz), theta (4–7 Hz), alpha (8–13 Hz), beta (14–30 Hz) |
| Wei et al. [16] | NuAmps 32 channel 500 Hz sampling | P8, T8, CP6, FC6, F8, F4, C4, P4, AF4, Fp2, Fp1, AF3, Fz, FC2, Cz, CP2, PO3, O1, Oz, O2, PO4, Pz, CP1, FC1, P3, C3, F3, F7, FC5, CP5, T7, P7 | 1–50 Hz (undefined) |
| Wei et al. [14] | NuAmps 32 channel 500 Hz sampling | P8, T8, CP6, FC6, F8, F4, C4, P4, AF4, Fp2, Fp1, AF3, Fz, FC2, Cz, CP2, PO3, O1, Oz, O2, PO4, Pz, CP1, FC1, P3, C3, F3, F7, FC5, CP5, T7, P7 | Delta (1–3 Hz), theta (4–7 Hz), alpha (8–12 Hz), beta (13–30 Hz), gamma (31–50 Hz) |
| Ko et al. [15] | NuAmps 32 channel 500 Hz sampling | FP1, FP2, C3, C4, Pz, Oz | 1–60 Hz |
| Lin et al. [17] | NuAmps 32 channel 500 Hz sampling | P8, T8, CP6, FC6, F8, F4, C4, P4, AF4, Fp2, Fp1, AF3, Fz, FC2, Cz, CP2, PO3, O1, Oz, O2, PO4, Pz, CP1, FC1, P3, C3, F3, F7, FC5, CP5, T7, P7 | Delta (0.1–3 Hz), theta (4–7 Hz), alpha (8–12 Hz), beta (13–20 Hz), gamma (21–50 Hz) |
| Ko et al. [18] | NuAmps 32 channel 500 Hz sampling | P8, T8, CP6, FC6, F8, F4, C4, P4, AF4, Fp2, Fp1, AF3, Fz, FC2, Cz, CP2, PO3, O1, Oz, O2, PO4, Pz, CP1, FC1, P3, C3, F3, F7, FC5, CP5, T7, P7 | Delta (0.1–3 Hz), theta (4–7 Hz), alpha (8–12 Hz), beta (13–20 Hz), gamma (21–30 Hz) |
| Lin et al. [19] | NuAmps 32 channel 500 Hz sampling | P8, T8, CP6, FC6, F8, F4, C4, P4, AF4, Fp2, Fp1, AF3, Fz, FC2, Cz, CP2, PO3, O1, Oz, O2, PO4, Pz, CP1, FC1, P3, C3, F3, F7, FC5, CP5, T7, P7 | Delta (0.1–3 Hz), theta (4–7 Hz), alpha (8–12 Hz), beta (13–20 Hz), gamma (21–30 Hz) |
| Pane et al. [26] | Emotiv Epoc + 14 channel 10/20 system 256 Hz | O1, O2 | Theta (4–8 Hz), alpha (8–12 Hz), beta (12–30 Hz) |
| Mawalid et al. [21] | Emotive Epoc + 14 10/20 system 256 Hz | AF3, F7, F3, FC5, T7, P7, O1, O2, P8, T8, FC6, F4, F8, AF4 | Alpha (8–13 Hz), beta (13–20 Hz) |
| Khoirunnisa et al. [20] | Emotiv Epoc + 14 channel 10/20 system 256 Hz | AF3, F7, F3, FC5, T7, P7, O1, O2, P8, T8, FC6, F4, F8, AF4 | Theta (4–8 Hz), alpha (8–16 Hz), and beta (16–32 Hz) |
| Dennison et al. [25] | Advanced Neuro Technologies 64 channel cap | All 64 with some removal and interpolation due to artifacts | Delta, theta, alpha, beta, and gamma bands (0.1–30 Hz), undefined power band ranges |
| Jeong et al. [22] | Emotiv Epoc + 14 channel 10/20 system 2048 Hz down-sampled upon export to 128 Hz | AF3, F7, F3, FC5, T7, P7, O1, O2, P8, T8, FC6, F4, F8, AF4 | Theta (4–8 Hz), alpha (8–12 Hz), low beta (12–16 Hz), high beta (16–25 Hz), gamma (25–45 Hz) |
| Li et al. [35] | Neuroscan SynAmps2 Model 8050 Eeg amplifier and data acquisition system. 64 channel 1000 Hz AC sampling | FP1, FP2, AF3, AF4, F3, F4, F7, F8, FZ, FC1, FC2, FC5, FC6, C3, C4, Cz, CP1, CP2, CP5, CP6, P3, P4, P6, P7, P8, Pz, PO3, PO4, O1, O2, Oz | Theta (4–8 Hz), alpha (8–13 Hz) |
| Kim et al. [42] | Eight channel 250 Hz, 16 bits | Undear | none |
| Liao et al. [27] | Neuroskymind wave mobile 512 Hz | FP1 | Broad band frequencies: delta, theta, low alpha, high alpha, low beta, high beta, low gamma, high gamma |
| Li et al. [23] | Opebci 256 Hz sampling 8 channel Ag/AgCl dry electrode brain cap | FP1, FP2, C3, C4, P3, P4, O1, O2 | Delta (0.5–3 Hz), theta (4–7 Hz), alpha (8–13 Hz), beta (14–30 Hz) |
| Lee and Alamaniotis [43] | Cognionics 10/20 system 32 channels, sometimes 64 channels was used, 256 or 512 Hz, respectively | Not reported | raw EEG |
| Recenti et al. [24] | AntNeuro 64-channel dry electrode cap 500 Hz | All 64 with some removal and interpolation due to artifacts | Delta (0.5–4 Hz), theta (4–8 Hz), alpha (8–13 Hz), beta (13–35 Hz), low gamma (35–40 Hz) |

(EDA), eye tracker, postural sway and body sensors at the head and waist. Derived variables include power band analysis of EEG [12–27], electrical potentials of eye movement from EOG [25, 28, 29], heart rate and heart rate variability measures from ECG [25, 28–33] which can also be calculated from blood volume pulse (BVP) obtained from PPG [32, 33], gastric activity from EGG [25, 29], muscle activity from EMG [24], respiration rate [25, 28–32], skin conductivity from GSR [28–31, 33], eye blinks [25, 28], weight shifts [25, 34] and center of pressure for postural sway [35], and head and waist movements from body sensors [25, 35].

3.7 Neural networks

Nam et al. [12] is the earliest known publication in the field of automatic detection of cybersickness. The study used a 2-layer feed-forward artificial neural network to partially detect nausea timings. Other studies used deep neural networks (DNN) [22], including multilayer perceptron (MLP) [35], radial basis function neural network (RBFNN) [14, 16], convolutional neural network (CNN) [42], recurrent neural network-long short term memory (RNN-LSTM) [27], as well as self-organizing neural fuzzy inference network (SONFIN) [19], and deep embedded self-organizing map (DESOM) with a CNN auto encoder and decoder from EEGnet [43].

DNNs are neural networks with two or more fully connected hidden layers, usually stacked linearly in groups. MLP and RBFNN are DNNs that differ in how their outputs are determined. MLP networks work globally and their outputs are decided by all neurons. In contrast, RBFNNs are local approximation networks whose outputs are determined by hidden units in local receptive fields. CNNs are also a type of DNN. They learn patterns in the data through filtering in convolutional layers, then pass data through pooling layers to compress the size of representation, allowing for parameters to be computed faster. CNNs are optimized for image data. RNNs are another type of DNN. They learn representations in an iterative manner, using outputs of a layer as recurrent inputs to the same or other layers. LSTMs are a subset of RNNs, that allow for the learning and reconstruction of signals, and allow for the prediction of future signals based on previous timesteps of data [27, 30, 31, 42]. SONFIN and DESOM are examples of self-organizing neural networks, that work based on weights between nodes.

3.8 Other ML tools

There are a variety of other non-neural network machine learning tools employed in the reviewed studies. These include: maximum gaussian likelihood estimator [13]; a simple tool that uses a gaussian distribution, where

maximum probability of a label occurs if the data points are closer to their mean value, support vector machines (SVM) which try and find the best hyperplane between data sets that belong to different classes [13, 18, 17], its variations with kernel functions of polynomial SVM [23], SVM-radial basis function (RBF) [20, 23], support vector regression (SVR) [16, 19], linear regression (LR) which assumes a linear relationship between input and output variables [15, 16, 19, 33], linear discriminant analysis (LDA) which finds linear combinations of features that can separate classes [20, 25], principle component regression (PCR) [15] based on principle component analysis, naïve bayes based on probability theorem [21], *k*-nearest neighbours (kNN) [13, 20, 21, 23, 25, 28, 32, 35, 43] which labels new data according to the majority of nearby pre-labelled data, decision trees that employ a flowchart-like structure for decision making [25, 26], including random forest [24, 35] and bagged decision tree which reduces the variance of a decision tree [25], gradient boosting trees to minimize errors [24], and CN2 rule induction that extracts rules from features in a data set [26]. Studies that have used these machine learning tools have detected but not predicted future cybersickness states.

3.9 Classification types

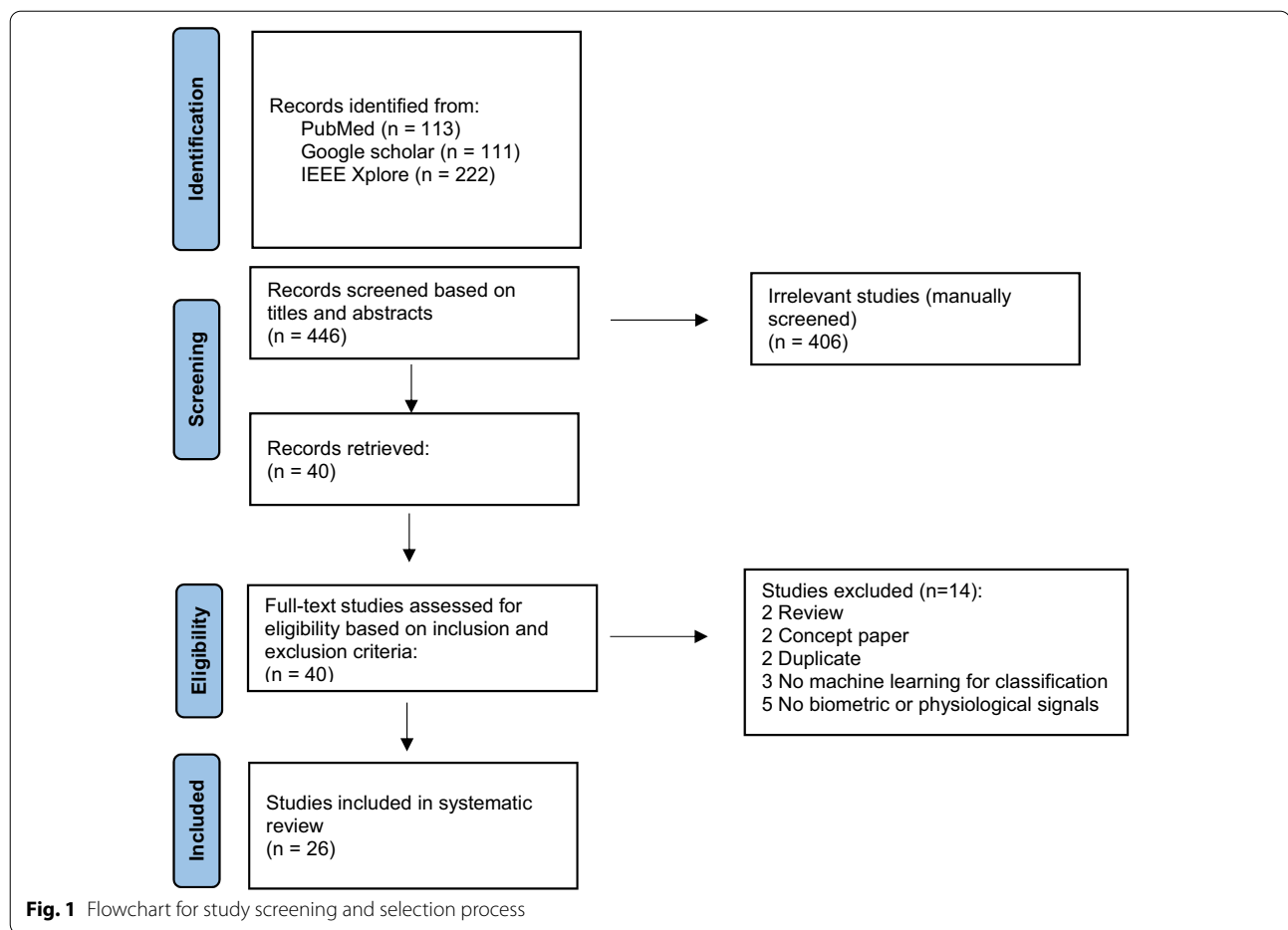
Some studies use a mix of binary and multiclass classification. Binary classification refers to the labelling of two different classes in a machine learning task, whereas multiclass classification refers to multiple labels, which in this review concerns levels of cybersickness severity. Other studies use machine learning to estimate simulator sickness questionnaire (SSQ) scores, which is another form of multiclassification.

3.10 Data selection

A summary of reporting styles, cybersickness and non-cybersickness data labelling is summarized in Table 6.

Multiple methods for choosing data segments related to cybersickness have been used. These include a report on the first instance of cybersickness perception [12, 43]. Commonly, entire video segments or VR immersion sessions were used if they had been labelled as cybersickness [20, 22, 27–32]. Specific timeframes were also picked. This is so that either cybersickness is highest or most likely at the selected data segment [18, 21, 26] to capture cybersickness intervals [23, 25, 35], or to predict future states using past data sectioned in various temporal window sizes [33].

The method of labelling data segments as ‘non-cybersickness’ varied among studies. Some studies choose to label ‘non-cybersickness’ as the beginning data segment while wearing an HMD, with a static image and no camera movement in the VR environment [35, 43]. Others



have opted to use data segments recorded before VR immersion or gameplay [20, 21, 23, 26, 31, 32]. Studies have also chosen to select data that does not meet different cutoffs using SSQs scores or rating scales [25, 28, 30, 33, 42]. Alternatively, chosen data samples were those with no report of cybersickness during VR immersion [27, 32], or data segments not corresponding to the cybersickness label [12]. In studies, where motion sickness levels were estimated, the ‘non-cybersickness’ labels and time segments were participant defined via a self-operated joystick scale, keeping note that the earliest timepoint of recording in these studies already included a moving video [13–19]. Several studies included in this review do not label data specifically as ‘non-cybersickness’. These consist of two studies that attempt to estimate SSQ scores [29, 34], while one tries to classify EEG, heart rate and EMG signals into specific binary indexes related to motion sickness [24]. Thus, the classification of ‘non-cybersickness’ data refers to participants in many different environments across studies, in terms of pre and during immersion states as well as exposure to movement and non-movement of visual scenes.

3.11 Preprocessing

Preprocessing refers to the manipulation of raw data so that specific variables can be generated for further processing. During preprocessing, methods are used to reduce redundancy and extract meaningful data. Methods include down sampling to reduce the amount of data, filters to remove artifacts and select only a portion of data, manual artifact correction, computational artifact correction, such as z-scores and independent component analysis (ICA), weighting data based on signal quality, data transformation using variations of Fast Fourier Transform (FFT), and optimization of fixed windowed time segments. This is summarized in Table 7.

3.12 Features extraction, selection and fusion

Feature extraction and selection is a method to get a subset of relevant features/variables from the data, to be fed as an input into a machine learning tool. The idea is to reduce complexity and feed algorithms with the most relevant data. Studies have focused on spatial locations of EEG channels, as well as temporal, frequency and amplitude variables from recorded biosignals. Methods

used range from manual selection to statistical computations, genetic algorithms, and convolutional networks. Most notably, three studies focus on selecting as few EEG channels as possible, showing that one to three channels can be used for cybersickness detection [20, 26, 27]. In addition to obtaining features, feature fusion allows data from multiple biometric and physiological signals to be combined for classification. Out of 26 studies, 13 studies have fused features from multiple signals. Feature extraction and selection techniques and details of studies that have applied feature fusion are displayed in Table 8.

3.13 Important features for classification

Important features (Table 8) were included according to the following criteria: correlation to cybersickness scores or by optimal classification accuracies, appearance in multiple machine learning models [25], and if eight or fewer channels are involved and named [12, 15, 23]. In cases, where the authors have not explicitly pointed out or done an analysis to rank the importance of features, all the features used in the classification are included in the list for transparency of information and comparison to other studies [12, 13, 16, 27, 32]. For a full compilation of EEG devices, channels and power band frequencies used in the reviewed studies, refer to Table 9. Frequency ranges for each power band are reported in Table 9 because of the inconsistencies between studies, especially in regard to differentiation of the beta and gamma bands.

Across reviewed studies, the overall importance of broad band EEG frequency signals is revealed; with a focus on alpha (8–12 Hz), beta (13–20 Hz) and gamma bands (21–30 Hz) in channels relating to cortical regions in occipital areas (O1, O2, Oz) [12, 15, 17–20, 23, 25, 26], parietal areas (P3, P4, Pz) [12, 15, 17, 18, 25, 42] and left and right frontal areas [15, 20, 23, 25].

Postural sway [24, 34, 35], head and body movement [25, 35] and blink rate [25, 28, 29] have shown to be useful features for cybersickness classification. Among others, heart rate has consistently been an important feature across studies [24, 25, 28, 30–33]. A heart rate variability (HRV) indicator, pNN50, which is the percentage of N–N intervals within 50 ms, has also been a high contributor to results obtained in both binary and multiclassification tasks [33]. Alongside ECG derived variables, respiration rate has been identified as an important feature for cybersickness classification and estimation [25, 28, 32]. Electrodermal activity also known as galvanic skin response has shown promise as an important feature in four studies [28, 30, 31, 33], but did not make a statistically significant correlation with SSQ scores in another [29].

4 Discussion

Overall, the type of population, and an assessment of algorithm utility remains ambiguous and wanting. The wide differences in study protocols, data labelling and processing make it difficult to compare the reviewed studies. Although scarce, the available studies have highlighted that it is possible to track cybersickness using a variety of biosignals. The robustness of these signals to noise in practical settings, however, requires careful consideration. Looking forward, the discovery of new information about cybersickness requires machine learning tools that are open and explainable. These aspects are discussed below.

4.1 Subject demographics

4.1.1 *The subject demographics are biased towards males, with a lack of age range reporting*

There is evidence that females tend to be more susceptible to visually-induced motion sickness than males [45]. Both vestibular and visual motion sickness incidence in females tends to be higher than in males, but with no difference in the severity of symptoms [46–49]. Emerging evidence suggests that interpupillary distance non-fit, while wearing HMDs is one driving factor for this gender discrepancy [50]. A meta-analysis of factors associated with cybersickness suggested that age may be a contributor to likelihood of sickness [51]. As much as possible, the gender demographic and age range should be reported as a means of identifying possible influences towards study results. Studies may want to balance or separate analyses of females and males. An argument could be made, however, that female and male analysis should be done together so that a machine learning model can be subject to a wide population and subject demographic.

4.2 Prediction versus detection

4.2.1 *Studies have presented evidence for the detection of cybersickness and further cybersickness events, but predictive capabilities for novel, first-instance cybersickness events are in question*

It is not necessarily the machine learning algorithm used that determines the model's ability to detect or predict cybersickness but the choice of data segments. Data segments in prediction studies have been chosen before the onset of cybersickness, allowing machine learning models to be trained on data prior to the future event. Training on prior data is inbuilt for studies using LSTMs, allowing researchers to specify timesteps of certain lengths as training for signal reconstruction of relative future timepoints [52]. However, studies do not specify the timing of cybersickness occurrence in each data sample, meaning that crossing

a certain timepoint, the model could be trained on data already related to cybersickness to detect future cybersickness events. This leads to the question: are the models truly predictors, detectors, or a combination of both? If indeed they are a combination, these models could be defined as a detection-based prediction model, in which current cybersick data can be used to predict future cybersick data. With the exception of Islam et al. [31], the literature lacks models only trained on clear non-cybersickness segments that are used to detect future cybersick events. Furthermore, literature so far has focused on detecting cybersickness events using data segments related to VR immersion, but few have tried to predict future cybersick events using pre-VR immersion baselines [31]. To the best of our knowledge, there is a lack of machine learning studies focused on predicting susceptibility or future cybersick events in VR using the normal resting physiological state of an individual.

4.3 Labelling

4.3.1 Labelling cybersick data in long windows could increase false positives and negatives

A drawback to labelling entire video segments or VR immersion sessions based on a post SSQ or on a first instance reporting basis is the lack of temporal precision. Large portions of data could in truth represent the wrong label, increasing rates of false positives and false negatives during classification. Where possible, a solution would be to have data segments that are in relatively small temporal windows, ideally near the time of reporting and to avoid large temporal windows in the order of minutes.

4.3.2 Non-cybersick data should be labelled under the same experimental conditions as cybersick data

If 'non-cybersickness' data is not under the same conditions as 'cybersick' labelled data, the risk increases that a machine learning algorithm learns the difference between conditions influenced by a different environment, rather than the perception of cybersickness itself.

4.4 The reviewed studies are difficult to compare

Stimulus type, environment and participant activity differ greatly across studies. Different stimuli inputs, as well as virtual environments and scene content, and standing and sitting conditions make studies difficult to compare. With regard to comparing EEG studies, vestibular stimuli and visual stimuli used to induce motion sickness activates a vast array of different cortical areas

in the brain [37, 53–62]. Previous research has also found that certain movements of visual scenes inside VR can alter HRV [8, 63]. Constant clockwise rotation of the visual environment has been found to inhibit cardiac parasympathetic activity [8]. Root mean square of successive differences of R-R intervals (RMSSD) and standard deviation of R-R intervals (SDRR), measures of parasympathetic activity, were also found to be decreased in forward visual movement compared to backward visual movement during VR immersion in a rollercoaster ride [63]. In addition, vestibular stimuli is known to increase cardiac sympathetic activity [64], meaning that different activity levels could potentially alter HRV variables and associated feature importance. Thus, on top of feature extraction and selection methods, extra care needs to be taken when deciding which features to choose for a new study.

4.5 Features

4.5.1 Parietal, occipital and frontal cortical areas in the alpha, beta and gamma band are highly related to cybersickness in machine learning studies

Gamma band signal importance for classification is in line with recent findings, showing increased gamma power with increased cybersickness severity [65]. In the application of frequency filters to reduce artifacts and noise, one should be careful not to filter out valuable information that could exist past chosen frequency boundaries.

It is also important to keep in mind that evidence for parietal and occipital feature importance in cybersickness stem mainly from two studies that either have considerably more vestibular stimuli through moving platforms or use desktop LED displays rather than VR HMDs [23, 25], and are thus different in environment and stimulation type. More research is needed as a cross reference to determine if these features are common regardless of environment or stimulation type.

Nevertheless, the involvement of multiple brain regions suggests that interactions and connections exist across different spatial locations. In an fMRI study by Toschi et al. [37], reduced connectivity was found in nausea states compared to baseline, between the right and left primary visual cortex (V1), as well as increased connectivity between the right middle temporal visual area (MT+/V5) and anterior insular, and between the left MT+/V5 and the middle cingulate cortex. Thus, deeper brain structures could be involved that may not necessarily be revealed in the above machine learning EEG studies.

4.5.2 None of the machine learning methods used so far have clearly revealed the complex, dynamic, spatio-temporal processes in the brain related to cybersickness

Studies have relied on statistical comparisons between sets of cybersickness and normal/control data, to find important frequency-based power spectra in isolated channels, or spatial clusters over large brain regions. Beyond this, communication between spatial locations, functional networks, and temporally relevant information still needs to be explored. More complex machine learning algorithms have not been employed for knowledge extraction. This important task requires new machine learning methods on its own.

4.5.3 Heart rate, heart rate variability, postural sway, head and body movement, blink rate, breathing rate and EDA are informative features

Important features of increased heart rate have been found to be correlated with increasing cybersickness severity [65]. Heart rate variability measures other than pNN50, like changes in the average duration of N–N intervals (AVGNN), and changes in the standard deviation of N–N intervals (STDNN) have been correlated with SSQ scores [66]. Head and body movement could potentially exacerbate sensory mismatches while in VR and is part of the generally accepted sensory mismatch theory [67]. The contribution of increased postural sway to detect cybersickness is rooted in the postural instability theory for motion sickness [68], although a study has shown a weak link between postural instability and cybersickness. Eye movements have also been hypothesized to generate motion sickness [69]. Blink rate seems likely a symptom of oculomotor disturbances, which is a subcategory for simulator sickness [70]. Breathing rate appears to be an important feature under experimental conditions [25, 28, 29, 32]. Furthermore, controlled diaphragmatic breathing has also been studied to manage cybersickness through modulation of the parasympathetic nervous system [71].

4.5.4 The fewer channels, the better

The number of channels is important for simplicity and ergonomic reasons. The fewer the channels, the less bulky an automated cybersickness detection or prediction system device needs to be. Using 64 channels [24, 25] is unwieldy outside of lab conditions in an operational or consumer setting. It also requires good signal quality from most, if not all channels. Therefore, it is suggested that studies investigate channel reduction methods while still preserving accuracy.

4.5.5 Features discovered from extraction and selection, or those that contribute the most to optimal classification accuracies, may not be generalizable or interpretable

While studies have drawn attention to many features, it is important to note that the most correlated features may not be the most frequently chosen by feature extraction/selection tools [14]. The generalizability of features to different experimental settings still needs to be assessed. This will help build a robust model of physiological activity during cybersickness events. Features related to cybersickness can also be statistically tested and compared to their importance in machine learning models. This can be a helpful indicator of their correlation versus importance. Finally, features obtained for novel, first-instance future cybersickness event prediction are predictive features. They may not necessarily be the same features occurring during cybersickness. Thus, caution is warranted as the same features listed in this review may not be generalizable to a study attempting to predict cybersickness from pre-immersion baselines.

4.5.6 Some forms of signal acquisition are more practical than others

VR content has been explored as a data source for cybersickness classification as well [42, 72]. Current interventions include narrowing the field of view or slightly changing the visual scene to attenuate cybersickness symptoms [73]. While virtual environment contents provide useful data in retrospect, they cannot be the medium for intervention in all situations. Such would be the case for high-stakes training simulations or even immersive real-time operations that require large fields of view and a high degree of realism. Unfortunately, even with live streaming, the predictive nature of virtual content would be limited without availability beforehand. VR content is a stimulus and cannot be used to directly assess individual cybersickness. Biometric and physiological signals, on the other hand, can measure human states and responses to both the environment and clinical treatment [74, 75]. Moreover, wearable devices are portable and can still be used while engaging with VR in a non-sedentary manner. This level of practicality and freedom is currently not possible with other forms of data capture such as with the brain (magnetoencephalography [76], functional magnetic resonance imaging [77]). Still, not all signals from wearable devices are as practical as each other. EEG, EOG, ECG, PPG, EGG and eye tracker could be used in combination for cybersickness detection and prediction in a practical consumer or operational setting. Respiration signals, GSR, postural sway and body movement, in

contrast, could be difficult to implement. In high activity settings, these signals may become riddled with artifact and noise (from heavy erratic breathing, profuse sweating, and large amounts of movement), reducing the practicality of these signals.

4.6 Future suggestions

Along with reporting of subject demographics, proper labelling of data and investigations of channel reduction methods to reduce the number of sensors needed to capture this data, there are several other future suggestions. The future of machine learning on cybersickness involves not just the alteration of visual displays for human ergonomic comfort, but the understanding of physiological states and subsequent mitigation of potentially harmful perceptual responses. Given the interactive nature of immersive technology, devices that capture data related to physiological states have to be wearable and not bulky or restraining while engaging in virtual reality. The field of cybersickness also requires more understanding, both on the mechanisms of how it originates and on the biomarkers through which this event can be either predicted or detected. One potential avenue of machine learning exploration could be to pair cybersickness along with other correlated or anticorrelated psychological aspects, such as vection [78] and presence [79], respectively.

Future studies could collect data from eyetrackers embedded in VR devices to track both gaze and fixation and fuse this with other already known biosignals [80]. Further on, building algorithms designed to process multiple signals in combination and independently would be especially useful in operational environments. If one source of data is cut off, another could take its place. This would maintain robust data streams for the monitorization of physiological states.

The next step in machine learning would be to generate new information every time new sample data is added (incremental, online learning) and to better model and explain related spatio-temporal brain processes. One way to do this would be to use a 3D evolving spiking neural network architecture [81, 82]. Considered the 3rd generation of artificial neural networks (ANN), spiking neural networks use spike information representation to account for changes in brain data and to learn spatio-temporal patterns from the data, which patterns can then be interpreted to understand the dynamics of the brain under certain conditions. This is in contrast to the 2nd generation ANNs, some of them reviewed above, which are not biologically plausible and do not reflect how neurons in the brain actually work in time and space under different conditions. ANNs are more computationally and energy intensive and less efficient in the interpretation of results. Perhaps, the biggest pitfall of deep neural network (DNN)-type algorithms is that they are 'black boxes' with many hidden layers, meaning that data

interpretation is limited [83]. A dynamic evolving spiking neural network is based on the concept of an evolving connectionist system [82]. It is a modular system that evolves both structure and functionality from incoming data, in a way that is continuous, self-organized, online adaptive and interactive [84]. This makes it possible to learn spatio-temporal brain data (STBD), and the actual machine learning architecture as an interpretable model of the brain. This is useful, because unlike DNNs, it allows researchers to then act on the modelling results in a meaningful way. Architectures like NeuCube are robust to noise and create an approximate map of structural and functional cortical areas of interest using EEG data [81]. The data can be used to interpret brain activity during cybersickness experiments. Open and explainable AI systems built on brain-inspired spiking neural networks would further pave the way for integrated cybersickness prevention and alleviation techniques through better neuro-physiological data modelling, biomarker discovery and deeper understanding of personalised cybersickness processes. From an industry perspective, this information will help producers of VR content understand their consumer more, and help lift barriers to non-contact training simulations in professional fields, gaming and the building of interactive digital economies. Finally, training for resistance to cybersickness based on both objective physiological data and subjective feedback will pave the way for human adaptation to an era of ever-increasing virtual environments.

5 Conclusions

This review of machine learning approaches in cybersickness studies demonstrated that a wide range of biometric and neuro-physiological signals for cybersickness identification have been analysed and discovered through the use of machine learning. Multiple machine learning architectures, modes of stimulus, VR content, environment, and participant activity have been used in studies for the automatic detection of cybersickness and prediction of further cybersick events based on these biomarkers. The predictive capabilities of current machine learning models for novel, first-instance cybersickness events, however, are still in question. Common important features have been highlighted that may be used as an input for future machine learning research in the field of cybersickness. Future research is pointed towards the collection of quality data, and the use of brain-inspired spiking neural network models [82] to achieve better accuracy and understanding of complex spatio-temporal brain processes related to cybersickness.

Appendix

See Table 10.

Table 10 Risk of bias (ROB) assessment for 26 development and validation studies judged based on the 20 signaling question items from PROBAST [41]

| Item | Paper code | | | | | | | | | | | | | | | | | | | | | | | | | |
|---|------------|-----|-----|-----|-----|-----|-----|-----|-----|-----|-----|-----|-----|-----|-----|-----|-----|-----|-----|-----|-----|-----|-----|-----|-----|-----|
| | 1 | 2 | 3 | 4 | 5 | 6 | 7 | 8 | 9 | 10 | 11 | 12 | 13 | 14 | 15 | 16 | 17 | 18 | 19 | 20 | 21 | 22 | 23 | 24 | 25 | 26 |
| <i>Participants and data sources</i> | | | | | | | | | | | | | | | | | | | | | | | | | | |
| 1 | Y | Y | Y | Y | Y | Y | Y | Y | Y | Y | Y | Y | Y | Y | Y | Y | Y | Y | Y | Y | Y | Y | Y | Y | Y | Y |
| 2 | Y | N | NI | NI | Y | Y | Y | Y | Y | PN | N | N | Y | Y | N | N | Y | Y | N | Y | PY | PY | PY | Y | PN | NI |
| <i>Definition and measurement of features used for classification</i> | | | | | | | | | | | | | | | | | | | | | | | | | | |
| 3 | Y | Y | Y | Y | Y | N | N | Y | Y | Y | Y | Y | Y | Y | Y | Y | Y | Y | Y | Y | Y | Y | Y | Y | Y | Y |
| 4 | Y | Y | Y | Y | Y | Y | Y | Y | Y | Y | Y | Y | Y | Y | Y | Y | Y | Y | Y | Y | Y | Y | Y | Y | Y | Y |
| 5 | Y | Y | Y | Y | Y | N | N | Y | Y | Y | Y | Y | Y | Y | Y | Y | Y | Y | Y | Y | Y | Y | Y | Y | Y | Y |
| <i>How and when the outcome of cybersickness was defined and determined</i> | | | | | | | | | | | | | | | | | | | | | | | | | | |
| 6 | Y | Y | Y | Y | Y | Y | Y | Y | Y | Y | Y | Y | Y | Y | Y | Y | Y | Y | Y | Y | Y | Y | Y | Y | Y | Y |
| 7 | Y | Y | Y | Y | Y | Y | Y | Y | Y | Y | Y | Y | Y | Y | Y | Y | Y | Y | Y | Y | Y | Y | Y | Y | Y | Y |
| 8 | Y | Y | Y | Y | Y | Y | Y | Y | Y | Y | Y | Y | Y | Y | Y | Y | Y | Y | Y | Y | Y | Y | Y | Y | Y | Y |
| 9 | Y | Y | Y | Y | Y | Y | Y | Y | Y | Y | Y | Y | Y | Y | Y | Y | Y | Y | Y | Y | Y | Y | Y | Y | Y | Y |
| 10 | Y | Y | Y | Y | Y | Y | Y | Y | Y | Y | Y | Y | Y | Y | Y | Y | Y | Y | Y | Y | Y | Y | Y | Y | Y | Y |
| 11 | Y | Y | Y | Y | Y | Y | Y | Y | Y | Y | Y | Y | Y | Y | Y | Y | Y | Y | Y | Y | Y | Y | Y | Y | Y | Y |
| <i>Statistical methods to develop and validate the model</i> | | | | | | | | | | | | | | | | | | | | | | | | | | |
| 12 | PN | N | N | N | N | N | N | N | N | N | N | N | N | N | Y | N | N | Y | Y | Y | N | N | N | Y | N | N |
| 13 | Y | Y | Y | Y | Y | Y | Y | Y | Y | Y | Y | Y | Y | Y | Y | Y | Y | Y | Y | Y | Y | Y | Y | Y | Y | Y |
| 14 | N | Y | Y | Y | Y | Y | Y | Y | Y | Y | Y | Y | Y | Y | Y | Y | Y | Y | Y | Y | Y | Y | Y | Y | Y | Y |
| 15 | NI | Y | Y | Y | Y | Y | Y | Y | Y | Y | Y | Y | Y | Y | Y | Y | Y | Y | Y | Y | Y | Y | Y | Y | Y | Y |
| 16 | Y | Y | Y | Y | Y | Y | Y | Y | N | Y | Y | Y | Y | Y | Y | Y | Y | Y | Y | Y | Y | Y | Y | Y | Y | Y |
| 17 | PY | Y | Y | Y | Y | Y | Y | Y | Y | Y | Y | Y | Y | Y | Y | Y | Y | Y | N | N | Y | Y | Y | Y | Y | Y |
| 18 | PY | Y | Y | Y | Y | Y | Y | Y | Y | Y | Y | Y | Y | Y | Y | Y | Y | Y | Y | Y | Y | Y | Y | Y | Y | Y |
| 19 | NI | PY | Y | Y | Y | Y | Y | Y | Y | Y | Y | Y | Y | Y | Y | Y | Y | Y | Y | Y | Y | Y | Y | Y | Y | Y |
| 20 | Y | Y | Y | Y | Y | Y | Y | Y | Y | Y | Y | Y | Y | Y | Y | Y | Y | Y | Y | Y | Y | Y | Y | Y | Y | Y |
| Overall ROB | low | low | low | low | low | low | low | low | low | low | low | low | low | low | low | low | low | low | low | low | low | low | low | low | low | low |

Papers are coded 1–26 from earliest to latest publication in the following order: 1. Nam et al. [12], 2. Yu et al. [13], 3. Wei et al. [14], 4. Wei et al. [16], 5. Ko et al. [15], 6. Lin et al. [17], 7. Ko et al. [18], 8. Lin et al. [19], 9. Dennison et al. [29], 10. Pane et al. [26], 11. Mawallid et al. [21], 12. Khoirunnisa et al. [20], 13. Dennison et al. [25], 14. Wang et al. [34], 15. Garcia-Agundez et al. [28], 16. Jeong et al. [22], 17. Li et al. [35], 18. Kim et al. [42], 19. Liao et al. [27], 20. Li et al. [23], 21. Lee and Alamaniotis [43], 22. Islam et al. [30], 23. Islam et al. [31], 24. Martin et al. [33], 25. Recenti et al. [24], 26. Oh and Kim [32]

Y = yes, PY = probably yes, N = no, PN = probably no, NI = no information

PROBAST 20 signalling question items:

Selection of participants and data sources used.

1. Were appropriate data sources used?
2. Were all inclusion/exclusions appropriate?

Definition and measurement of features used for classification.

3. Were predictors defined and assessed in a similar way for all participants?
4. Were predictor assessments made without knowledge of outcome data?
5. Are all predictors available at the time the model is intended to be used?

How and when the outcome of cybersickness was defined and determined.

6. Was the outcome determined appropriately?
7. Was a pre-specified or standard outcome definition used?
8. Were predictors excluded from the outcome definition?
9. Was the outcome defined and determined in a similar way for all participants?
10. Was the outcome determined without knowledge of predictor information?
11. Was the time interval between predictor assessment and outcome determined appropriate?

Statistical methods to develop and validate the model.

12. Were there a reasonable number of participants with the outcome?
13. Were continuous and categorical predictors handled appropriately?
14. Were all enrolled participants included in the analysis?
15. Were participants with missing data handled appropriately?
16. Was selection of predictors based on univariable analysis avoided?
17. Were complexities in the data accounted for appropriately?
18. Were relevant model performance measures evaluated appropriately?
19. Were model overfitting and optimism in model performance accounted for?
20. Do predictors and their assigned weights reported in the final model correspond to the rest of the analysis?

Acknowledgements

Not applicable.

Authors' contributions

YOC, NK, AXHY developed the concept. AXHY performed the literature review and wrote the draft. YOC, AXHY, and NK analyzed the literature and wrote and edited the main manuscript. All authors read and approved the final manuscript.

Funding

Not applicable.

Availability of data and materials

Not applicable.

Code availability

Not applicable.

Declarations**Ethics approval and consent to participate**

Not applicable.

Consent for publication

Consent from the authors of this review has been given for publication.

Competing interests

The authors declare that they have no competing interests.

Author details

¹Department of Anatomy, University of Otago, Dunedin, New Zealand. ²KEDRI, School of Engineering, Computer and Mathematical Sciences, Auckland University of Technology, Auckland, New Zealand. ³George Moore Chair of Data Analytics, Ulster University, Londonderry, UK. ⁴ABI, The University of Auckland, Auckland, New Zealand. ⁵Medtech Core NZ, Auckland, New Zealand. ⁶Brain Health Research Centre, Dunedin, New Zealand. ⁷Centre for Health Systems and Technology, Dunedin, New Zealand. ⁸Centre for Bioengineering and Nanotechnology, Point-of-Care Technologies Theme, University of Otago, Dunedin, New Zealand.

Received: 3 June 2022 Accepted: 15 September 2022

Published online: 09 October 2022

References

1. Davis S, Nesbitt K, Nalivaiko E (2014) A systematic review of cybersickness. In: Proceedings of the 2014 conference on interactive entertainment, pp 1–9. <https://doi.org/10.1145/2677758.2677780>
2. Zyda M (2005) From visual simulation to virtual reality to games. *Computer* 38(9):25–32
3. Sk R, Mallam SC, Nazir S (2021) Effectiveness of VR head mounted displays in professional training: a systematic review. *Technol Knowl Learn*. <https://doi.org/10.1007/s10758-020-09489-9>
4. Song H, Chen F, Peng Q, Zhang J, Gu P (2018) Improvement of user experience using virtual reality in open-architecture product design. *Proc Inst Mech Eng Part B J Eng Manuf* 232(13):2264–2275
5. Kim H, Kim DJ, Kim S, Chung WH, Park K-A, Kim JDK, Kim D, Kim MJ, Kim K, Jeon HJ (2021) Effect of virtual reality on stress reduction and change of physiological parameters including heart rate variability in people with high stress: an open randomized crossover trial. *Front Psychiatry*. <https://doi.org/10.3389/fpsy.2021.614539>
6. Boeldt D, McMahon E, McFaul M, Greenleaf W (2019) Using virtual reality exposure therapy to enhance treatment of anxiety disorders: identifying areas of clinical adoption and potential obstacles. *Front Psychiatry*. <https://doi.org/10.3389/fpsy.2019.00773>
7. Kothgassner OD, Goreis A, Kafka JX, Van Eickels RL, Plener PL, Felhofer A (2019) Virtual reality exposure therapy for posttraumatic stress disorder

- (PTSD): a meta-analysis. *Eur J Psychotraumatol* 10(1):1654782–1654782. <https://doi.org/10.1080/2008198.2019.1654782>
8. Yang AHX, Khwaounjoo P, Cakmak YO (2021) Directional effects of whole-body spinning and visual flow in virtual reality on vagal neuromodulation. *J Vestib Res*. <https://doi.org/10.3233/ves-201574>
 9. Ball C, Huang K-T, Francis J (2021) Virtual reality adoption during the COVID-19 pandemic: a uses and gratifications perspective. *Telem Inform* 65:101728. <https://doi.org/10.1016/j.tele.2021.101728>
 10. Lee L-H, Braud T, Zhou P, Wang L, Xu D, Lin Z, Kumar A, Bermejo C, Hui P (2021) All one needs to know about metaverse: a complete survey on technological singularity. *Virtual Ecosyst Res Agenda*. <https://doi.org/10.13140/RG.2.2.11200.05124/8>
 11. Kim H, Kim DJ, Chung WH, Park K-A, Kim JDK, Kim D, Kim K, Jeon HJ (2021) Clinical predictors of cybersickness in virtual reality (VR) among highly stressed people. *Sci Rep* 11(1):12139. <https://doi.org/10.1038/s41598-021-91573-w>
 12. Nam YH, Kim YY, Kim HT, Ko HD, Park KS (2001) Automatic detection of nausea using bio-signals during immersion in a virtual reality environment. In: 2001 conference proceedings of the 23rd annual international conference of the IEEE engineering in medicine and biology society. <https://doi.org/10.1109/IEMBS.2001.1020626>
 13. Yu Y, Lai P, Ko L, Chuang C, Kuo B, Lin C (2010) An EEG-based classification system of Passenger's motion sickness level by using feature extraction/selection technologies. In: The 2010 international joint conference on neural networks (IJCNN), pp 1–6. <https://doi.org/10.1109/IJCNN.2010.5596739>
 14. Wei C, Ko L, Chuang S, Jung T, Lin C (2011) Genetic feature selection in EEG-based motion sickness estimation. In: The 2011 international joint conference on neural networks, pp 365–369. <https://doi.org/10.1109/IJCNN.2011.6033244>
 15. Ko L-W, Wei C-S, Chen S-A, Lin C-T (2011) EEG-based motion sickness estimation using principal component regression. *Neural Inform Process*, pp 717–724
 16. Wei C, Ko L, Chuang S, Jung T, Lin C (2011) EEG-based evaluation system for motion sickness estimation. In: 2011 5th international IEEE/EMBS conference on neural engineering, pp 100–103. <https://doi.org/10.1109/NER.2011.5910498>
 17. Lin C, Tsai S, Lee H, Huang H, Ho S, Ko L (2012) Motion sickness estimation system. In: The 2012 international joint conference on neural networks (IJCNN), pp 1–6. <https://doi.org/10.1109/IJCNN.2012.6252580>
 18. Ko L, Lee H, Tsai S, Shih T, Chuang Y, Huang H, Ho S, Lin C (2013) EEG-based motion sickness classification system with genetic feature selection. In: 2013 IEEE symposium on computational intelligence, cognitive algorithms, mind, and brain (CCMB), pp 158–164. <https://doi.org/10.1109/CCMB.2013.6609180>
 19. Lin C, Tsai S, Ko L (2013) EEG-based learning system for online motion sickness level estimation in a dynamic vehicle environment. *IEEE Trans Neural Netw Learn Syst* 24(10):1689–1700. <https://doi.org/10.1109/TNNLS.2013.2275003>
 20. Khoirunnisa AZ, Pane ES, Wibawa AD, Purnomo MH (2018) Channel selection of EEG-based cybersickness recognition during playing video game using correlation feature selection (CFS). In: 2018 2nd international conference on biomedical engineering (IBIOMED), pp 48–53. <https://doi.org/10.1109/IBIOMED.2018.8534877>
 21. Mawali MA, Khoirunnisa AZ, Purnomo MH, Wibawa AD (2018) Classification of EEG signal for detecting cybersickness through time domain feature extraction using Naöve Bayes. In: 2018 international conference on computer engineering, network and intelligent multimedia (CENIM), pp 29–34
 22. Jeong D, Yoo S, Yun J (2019) Cybersickness analysis with EEG using deep learning algorithms. In: 2019 IEEE conference on virtual reality and 3D user interfaces (VR), pp 827–835. <https://doi.org/10.1109/VR.2019.8798334>
 23. Li X, Zhu C, Xu C, Zhu J, Li Y, Wu S (2020) VR motion sickness recognition by using EEG rhythm energy ratio based on wavelet packet transform. *Comput Methods Programs Biomed* 188:105266. <https://doi.org/10.1016/j.cmpb.2019.105266>
 24. Recenti M, Ricciardi C, Aubonnet R, Picone I, Jacob D, Svansson HÁR, Agnarssdóttir S, Karlsson GH, Baeringsdóttir V, Petersen H, Gargiulo P (2021) Toward predicting motion sickness using virtual reality and a moving platform assessing brain, muscles, and heart signals. *Front Bioeng Biotechnol*. <https://doi.org/10.3389/fbioe.2021.635661>
 25. Dennison M, D'Zmura M, Harrison A, Lee M, Raglin A (2019) Improving motion sickness severity classification through multi-modal data fusion, vol 11006. SPIE Defense + Commercial Sensing. SPIE
 26. Pane ES, Khoirunnisa AZ, Wibawa A, Purnomo MH (2018) Identifying severity level of cybersickness from EEG signals using CN2 rule induction algorithm. In: 2018 international conference on intelligent informatics and biomedical sciences (ICIIBMS), vol 3, pp 170–176
 27. Liao C, Tai S, Chen R, Hendry H (2020) Using EEG and deep learning to predict motion sickness under wearing a virtual reality device. *IEEE Access* 8:126784–126796. <https://doi.org/10.1109/ACCESS.2020.3008165>
 28. Garcia-Agundez A, Reuter C, Becker H, Konrad R, Caserman P, Miede A, Göbel S (2019) Development of a classifier to determine factors causing cybersickness in virtual reality environments. *Games Health J* 8(6):439–444. <https://doi.org/10.1089/g4h.2019.0045>
 29. Dennison MS, Wisti AZ, D'Zmura M (2016) Use of physiological signals to predict cybersickness. *Displays* 44:42–52. <https://doi.org/10.1016/j.displa.2016.07.002>
 30. Islam R, Lee Y, Jaloli M, Muhammad I, Zhu D, Quarles J (2020) Automatic detection of cybersickness from physiological signal in a virtual roller coaster simulation. In: 2020 IEEE conference on virtual reality and 3D user interfaces abstracts and workshops (VRW), pp 648–649. <https://doi.org/10.1109/VRW50115.2020.00175>
 31. Islam R, Lee Y, Jaloli M, Muhammad I, Zhu D, Rad P, Huang Y, Quarles J (2020) Automatic detection and prediction of cybersickness severity using deep neural networks from user's physiological signals. In: 2020 IEEE international symposium on mixed and augmented reality (ISMAR), pp 400–411. <https://doi.org/10.1109/ISMAR50242.2020.00066>
 32. Oh S, Kim D-K (2021) Machine-deep-ensemble learning model for classifying cybersickness caused by virtual reality immersion. *Cyberpsychol Behav Soc Netw*. <https://doi.org/10.1089/cyber.2020.0613>
 33. Martin N, Mathieu N, Pallamin N, Ragot M, Diverrez JM (2020) Virtual reality sickness detection: an approach based on physiological signals and machine learning. In: 2020 IEEE international symposium on mixed and augmented reality (ISMAR), pp 387–399. <https://doi.org/10.1109/ISMAR50242.2020.00065>
 34. Wang Y, Chardonnet JR, Merienne F (2019) VR sickness prediction for navigation in immersive virtual environments using a deep long short term memory model. In: 2019 IEEE conference on virtual reality and 3D user interfaces (VR), pp 1874–1881. <https://doi.org/10.1109/VR.2019.8798213>
 35. Li Y, Liu A, Ding L (2019) Machine learning assessment of visually induced motion sickness levels based on multiple biosignals. *Biomed Signal Process Control* 49:202–211. <https://doi.org/10.1016/j.bspc.2018.12.007>
 36. Yildirim C (2020) A review of deep learning approaches to EEG-based classification of cybersickness in virtual reality. In: 2020 IEEE international conference on artificial intelligence and virtual reality (AIVR), pp 351–357
 37. Toschi N, Kim J, Sclocco R, Duggento A, Barbieri R, Kuo B, Napadow V (2017) Motion sickness increases functional connectivity between visual motion and nausea-associated brain regions. *Auton Neurosci* 202:108–113. <https://doi.org/10.1016/j.autneu.2016.10.003>
 38. Krokos E, Varshney A (2021) Quantifying VR cybersickness using EEG. *Virtual Reality*. <https://doi.org/10.1007/s10055-021-00517-2>
 39. Page MJ, McKenzie JE, Bossuyt PM, Boutron I, Hoffmann TC, Mulrow CD, Shamseer L, Tetzlaff JM, Akl EA, Brennan SE, Chou R, Glanville J, Grimshaw JM, Hróbjartsson A, Lalu MM, Li T, Loder EW, Mayo-Wilson E, McDonald S, McGuinness LA, Stewart LA, Thomas J, Tricco AC, Welch VA, Whiting P, Moher D (2021) The PRISMA 2020 statement: an updated guideline for reporting systematic reviews. *BMJ* 372:n71. <https://doi.org/10.1136/bmj.n71>
 40. Moher D, Liberati A, Tetzlaff J, Altman DG, The PG (2009) Preferred reporting items for systematic reviews and meta-analyses: the PRISMA statement. *PLOS Med* 6(7):e1000097. <https://doi.org/10.1371/journal.pmed.1000097>
 41. Wolff RF, Moons KGM, Riley RD, Whiting PF, Westwood M, Collins GS, Reitsma JB, Kleijnen J, Mallett S (2019) PROBAST: a tool to assess the risk of bias and applicability of prediction model studies. *Ann Internal Med* 170(1):51–58. <https://doi.org/10.7326/M18-1376>

42. Kim J, Kim W, Oh H, Lee S, Lee S (2019) A deep cybersickness predictor based on brain signal analysis for virtual reality contents. In: 2019 IEEE/CVF international conference on computer vision (ICCV), pp 10579–10588. <https://doi.org/10.1109/ICCV.2019.01068>
43. Lee Y, Alamaniotis M (2020) Unsupervised EEG cybersickness prediction with deep embedded self organizing map. In: 2020 IEEE 20th international conference on bioinformatics and bioengineering (BIBE), pp 538–542. <https://doi.org/10.1109/BIBE50027.2020.00093>
44. Dennison MS, D'Zmura M (2017) Cybersickness without the wobble: experimental results speak against postural instability theory. *Appl Ergon* 58:215–223. <https://doi.org/10.1016/j.apergo.2016.06.014>
45. Kennedy R, Lanham D, Massey C, Drexler J, Lilienthal M (1995) Gender differences in simulator sickness incidence: implications for military virtual reality systems. *Safe J* 25(1):69–76
46. Klosterhalfen S, Pan F, Kellermann S, Enck P (2006) Gender and race as determinants of nausea induced by circular vection. *Gend Med* 3(3):236–242. [https://doi.org/10.1016/s1550-8579\(06\)80211-1](https://doi.org/10.1016/s1550-8579(06)80211-1)
47. Park AH, Hu S (1999) Gender differences in motion sickness history and susceptibility to optokinetic rotation-induced motion sickness. *Aviat Space Environ Med* 70(11):1077–1080
48. Graeber DA, Stanney KM (2002) Gender differences in visually induced motion sickness. *Proc Human Factors Ergon Soc Annu Meet* 46(26):2109–2113. <https://doi.org/10.1177/154193120204602602>
49. Cheung B, Hofer K (2003) Lack of gender difference in motion sickness induced by vestibular Coriolis cross-coupling. *J Vestibul Res* 12:191–200. <https://doi.org/10.3233/VES-2003-12405>
50. Stanney K, Fidopiastis C, Foster L (2020) Virtual reality is sexist: but it does not have to be. *Front Robot AI*. <https://doi.org/10.3389/frobt.2020.00004>
51. Saredakis D, Szpak A, Birkhead B, Keage HAD, Rizzo A, Loetscher T (2020) Factors associated with virtual reality sickness in head-mounted displays: a systematic review and meta-analysis. *Front Hum Neurosci*. <https://doi.org/10.3389/fnhum.2020.00096>
52. Sherstinsky A (2020) Fundamentals of recurrent neural network (RNN) and long short-term memory (LSTM) network. *Phys D Nonlinear Phenomena* 404:132306. <https://doi.org/10.1016/j.physd.2019.132306>
53. Van Ombergen A, Heine L, Jillings S, Roberts RE, Jeurissen B, Van Rompaey V, Mucci V, Vanhecke S, Sijbers J, Vanhevel F, Sunaert S, Bahri MA, Parizel PM, Van de Heyning PH, Laureys S, Wuyts FL (2017) Altered functional brain connectivity in patients with visually induced dizziness. *Neuroimage Clin* 14:538–545. <https://doi.org/10.1016/j.nicl.2017.02.020>
54. Chuang S-W, Chuang C-H, Yu Y-H, King J-T, Lin C-T (2016) EEG alpha and gamma modulators mediate motion sickness-related spectral responses. *Int J Neural Syst* 26(02):1650007. <https://doi.org/10.1142/s0129065716500076>
55. Dieterich M, Bense S, Stephan T, Yousry TA, Brandt T (2003) fMRI signal increases and decreases in cortical areas during small-field optokinetic stimulation and central fixation. *Exp Brain Res* 148(1):117–127. <https://doi.org/10.1007/s00221-002-1267-6>
56. Dieterich M, Bucher SF, Seelos KC, Brandt T (1998) Horizontal or vertical optokinetic stimulation activates visual motion-sensitive, ocular motor and vestibular cortex areas with right hemispheric dominance. An fMRI study. *Brain* 121(Pt 8):1479–1495. <https://doi.org/10.1093/brain/121.8.1479>
57. Della-Justina HM, Gamba HR, Lukasova K, Nucci-da-Silva MP, Winkler AM, Amaro E Jr (2015) Interaction of brain areas of visual and vestibular simultaneous activity with fMRI. *Exp Brain Res* 233(1):237–252. <https://doi.org/10.1007/s00221-014-4107-6>
58. Kleinschmidt A, Thilo KV, Büchel C, Gresty MA, Bronstein AM, Frackowiak RS (2002) Neural correlates of visual-motion perception as object- or self-motion. *Neuroimage* 16(4):873–882. <https://doi.org/10.1006/nimg.2002.1181>
59. Schmäl F (2013) Neuronal mechanisms and the treatment of motion sickness. *Pharmacology* 91(3–4):229–241. <https://doi.org/10.1159/000350185>
60. Chen YC, Duann JR, Chuang SW, Lin CL, Ko LW, Jung TP, Lin CT (2010) Spatial and temporal EEG dynamics of motion sickness. *Neuroimage* 49(3):2862–2870. <https://doi.org/10.1016/j.neuroimage.2009.10.005>
61. Frank SM, Baumann O, Mattingley JB, Greenlee MW (2014) Vestibular and visual responses in human posterior insular cortex. *J Neurophysiol* 112(10):2481–2491. <https://doi.org/10.1152/jn.00078.2014>
62. Smith AT, Wall MB, Thilo KV (2012) Vestibular inputs to human motion-sensitive visual cortex. *Cereb Cortex* 22(5):1068–1077. <https://doi.org/10.1093/cercor/bhr179>
63. Mazloumi Gavvani A, Hodgson DM, Nalivaiko E, Gavvani AM (2017) Effects of visual flow direction on signs and symptoms of cybersickness. *PLoS ONE* 12(8):e0182790–e0182790. <https://doi.org/10.1371/journal.pone.0182790>
64. Yates BJ, Bolton PS, Macefield VG (2014) Vestibulo-sympathetic responses. *Comprehens Physiol* 4(2):851–887. <https://doi.org/10.1002/cphy.c130041>
65. Lin Y-T, Chien Y-Y, Wang H-H, Lin F-C, Huang Y-P (2018) 65–3: the quantization of cybersickness level using EEG and ECG for virtual reality head-mounted display. *SID Sympos Digest Techn Pap* 49(1):862–865. <https://doi.org/10.1002/sdtp.12267>
66. García-Agundez A, Reuter C, Caserman P, Konrad R, Göbel S (2019) Identifying cybersickness through heart rate variability alterations. *Int J Virtual Real* 19(1):1–10. <https://doi.org/10.20870/IJVR.2019.19.1.2907>
67. Reason JT, Brand JJ (1975) Motion sickness. Academic Press, London
68. Riccio GE, Stoffregen TA (1991) An ecological theory of motion sickness and postural instability. *Ecol Psychol* 3(3):195–240. https://doi.org/10.1207/s15326969eco0303_2
69. Ebenholtz SM, Cohen MM, Linder BJ (1994) The possible role of nystagmus in motion sickness: a hypothesis. *Aviation Space Environ Med* 65(11):1032–1035
70. Kennedy RS, Lane NE, Berbaum KS, Lilienthal MG (1993) Simulator sickness questionnaire: an enhanced method for quantifying simulator sickness. *Int J Aviation Psychol* 3(3):203–220. https://doi.org/10.1207/s15327108ijap0303_3
71. Russell ME, Hoffman B, Stromberg S, Carlson CR (2014) Use of controlled diaphragmatic breathing for the management of motion sickness in a virtual reality environment. *Appl Psychophysiol Biofeedback* 39(3–4):269–277. <https://doi.org/10.1007/s10484-014-9265-6>
72. Padmanaban N, Ruban T, Sitzmann V, Norcia A, Wetzstein G (2018) Towards a machine-learning approach for sickness prediction in 360° stereoscopic videos. In: IEEE transactions on visualization and computer graphics, pp 1–1. <https://doi.org/10.1109/TVCG.2018.2793560>
73. Stanney K, Lawson BD, Rokers B, Dennison M, Fidopiastis C, Stoffregen T, Weech S, Fulvio JM (2020) Identifying causes of and solutions for cybersickness in immersive technology: reformulation of a research and development agenda. *Int J Hum Comput Interact* 36(19):1783–1803. <https://doi.org/10.1080/10447318.2020.1828535>
74. Thair H, Holloway AL, Newport R, Smith AD (2017) Transcranial direct current stimulation (tDCS): a beginner's guide for design and implementation. *Front Neurosci*. <https://doi.org/10.3389/fnins.2017.00641>
75. Constantinescu V, Matei D, Constantinescu I, Cuciureanu DI (2019) Heart rate variability and vagus nerve stimulation in epilepsy patients. *Transl Neurosci* 10:223–232. <https://doi.org/10.1515/tnsci-2019-0036>
76. Gross J (2019) Magnetoencephalography in cognitive neuroscience: a primer. *Neuron* 104(2):189–204. <https://doi.org/10.1016/j.neuron.2019.07.001>
77. Logothetis NK (2008) What we can do and what we cannot do with fMRI. *Nature* 453(7197):869–878. <https://doi.org/10.1038/nature06976>
78. Nooij SAE, Pretto P, Oberfeld D, Hecht H, Bülthoff HH (2017) Vection is the main contributor to motion sickness induced by visual yaw rotation: implications for conflict and eye movement theories. *PLoS ONE* 12(4):e0175305. <https://doi.org/10.1371/journal.pone.0175305>
79. Weech S, Kenny S, Barnett-Cowan M (2019) Presence and cybersickness in virtual reality are negatively related: a review. *Front Psychol* 10:158. <https://doi.org/10.3389/fpsyg.2019.00158>
80. Nam Y, Hong U, Chung H, Noh SR (2022) Eye movement patterns reflecting cybersickness: evidence from different experience modes of a virtual reality game. *Cyberpsychol Behav Soc Netw* 25(2):135–139. <https://doi.org/10.1089/cyber.2021.0167>
81. Kasabov NK (2014) NeuCube: a spiking neural network architecture for mapping, learning and understanding of spatio-temporal brain data. *Neural Netw* 52:62–76. <https://doi.org/10.1016/j.neunet.2014.01.006>
82. Kasabov NK (2018) Time-space, spiking neural networks and brain-inspired artificial intelligence (springer series on bio- and neurosystems). Springer

83. Tan C, Šarlija M, Kasabov N (2020) Spiking neural networks: background, recent development and the NeuCube architecture. *Neural Process Lett* 52(2):1675–1701. <https://doi.org/10.1007/s11063-020-10322-8>
84. Kasabov NK (2007) *Evolving connectionist systems: the knowledge engineering approach*. Springer, Berlin

Publisher's Note

Springer Nature remains neutral with regard to jurisdictional claims in published maps and institutional affiliations.

Submit your manuscript to a SpringerOpen[®] journal and benefit from:

- Convenient online submission
- Rigorous peer review
- Open access: articles freely available online
- High visibility within the field
- Retaining the copyright to your article

Submit your next manuscript at ► [springeropen.com](https://www.springeropen.com)